Chapter 5

Synthesis, *In-Vitro* Anti-Diabatic Activity, ADMET Properties and Molecular Docking Studies of Novel Thiazole Derivative

5.1. Introduction

Proteins are essential to biological systems because they act as structural components, regulators, and catalysts for a variety of cellular functions[153]. Enzymes in particular are notable for their extraordinary capacity to accelerate biological reactions, which facilitates vital metabolic pathways that are vital to life. α-amylase is an enzyme that holds great significance. A crucial part of the metabolism of carbohydrates is played by the protein enzyme α-amylase, which breaks down complex polysaccharides to simple sugars. Due to its exceptional catalytic capacity, it can cleave α-1,4-glycosidic bonds present in starch and glycogen, producing dextrins, maltotriose and maltose[154]. α-amylase is a ubiquitous protein found in many microbiological kingdoms, animal and plant. It is essential to many biological functions as well as industrial operations. α-amylase has been shown to catalyze the hydrolysis of glycosidic linkages by acid-base catalysis, which it enables through its catalytic site. A comprehensive comprehension of the interaction between α-amylase's structure and function is crucial, as it reveals the enzyme's numerous biological roles and helps to improve its industrial uses.

Thiazole is a heterocyclic molecule classified by having a five-membered ring structure that includes sulfur and nitrogen atoms. Heterocyclic molecules are essential to organic chemistry and are important in the material sciences, medicines, and many biological activities. Because of its wide variety of molecules, the five-membered ring is a fundamental building block for the synthesis of many different organic molecules. Because of its distinct structural properties, thiazole in particular attracts interest in pharmaceutical chemistry, materials science and agrochemicals. Its application in the fields of medication research and discovery is demonstrated by its inclusion into physiologically active molecules[155]. A wide range of biological actions, such as anticancer[156], antioxidant[157], anti-malarial activity[158], antibacterial[159], anticonvulsant[160], antimicrobial[161], antitumor[162],

antiproliferative[163], antidiabetic activity[140], antifungal[164], antitubercular[165], anti-inflammatory qualities[166], have been demonstrated by thiazole derivatives, making them attractive candidates for further research and development. Therefore, an understanding of the chemistry and uses of thiazole molecules is crucial for both industrial and research applications.

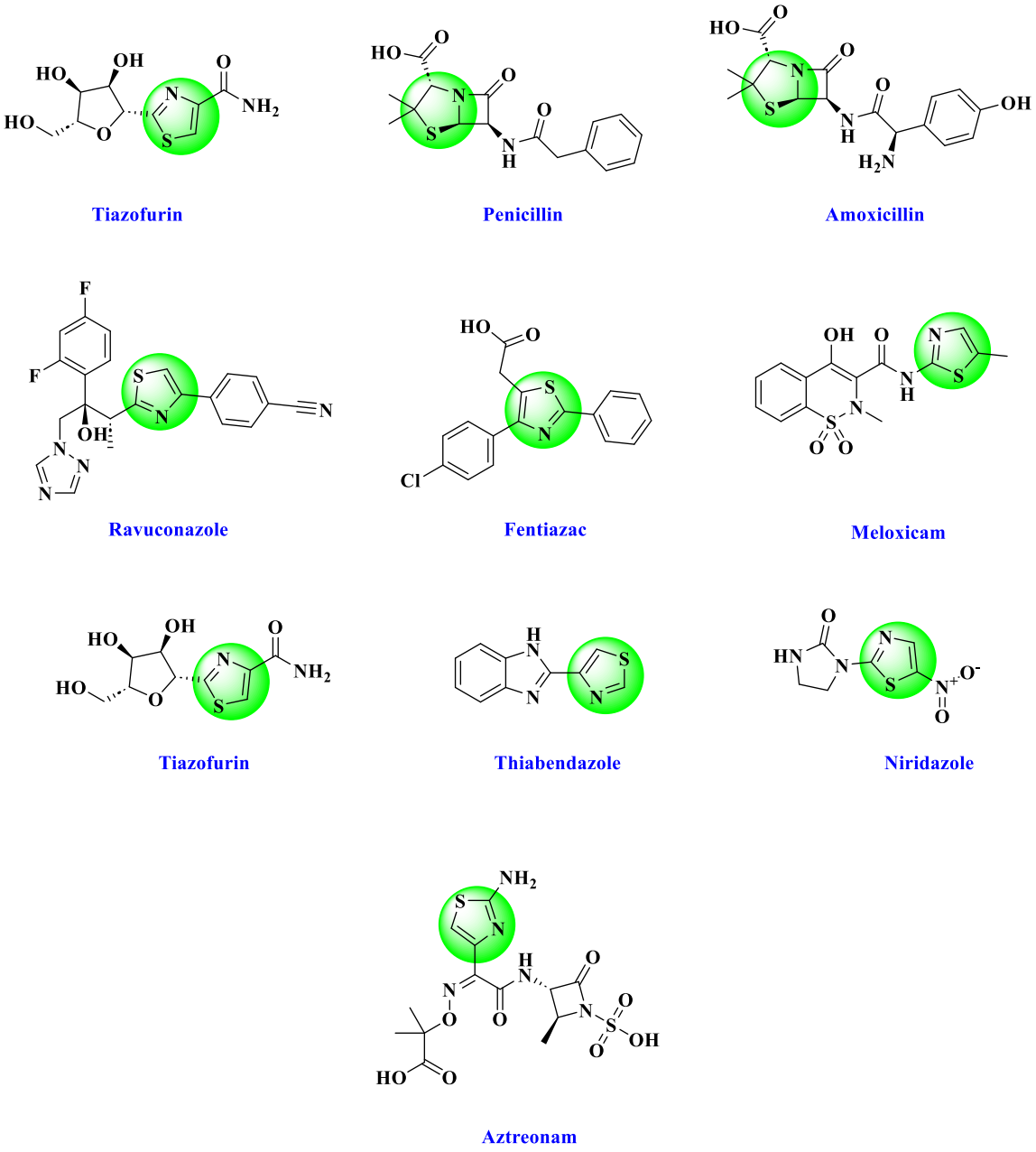

Scheme 1. Some thiazole-based synthetic commercial drug in the market.

5.1.1. Synthetic methods for substituted thiazole scaffold and its biological significance.

The synthesis of thiazole derivatives **3** was described by K. Childers *et al*[167]. Several aldehydes **1** underwent reactions with amino cyan acetamide **2** and sulphur in the presence of a base. The mixture was then refluxed in alcohol, resulting in the formation of thiazole derivatives **3** with amino carboxamide functionality **(Scheme 5.1)**.

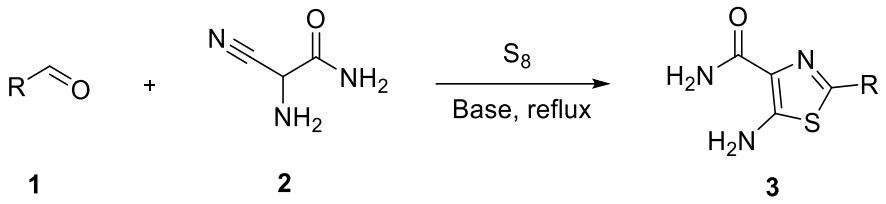

Scheme 5.1

The synthesis of new thiazole derivatives was described by A. Naggar *et al*[168], and it was an environmentally friendly process that involved reacting thiosemicarbazide **5** with acetyl thiophene **4** to generate compound **6**. Moreover, new thiazole compounds **7**, **8**, and **9** were created by the reaction of compound **6** with phenacyl bromide, chloro acetone and 3-nitro phenacyl bromide. When the synthesized compounds were tested for anticancer effects, it was found that methoxy group on the ring of phenyl had high inhibitory effect against a variety of cancerous cell types **(Scheme 5.2)**.

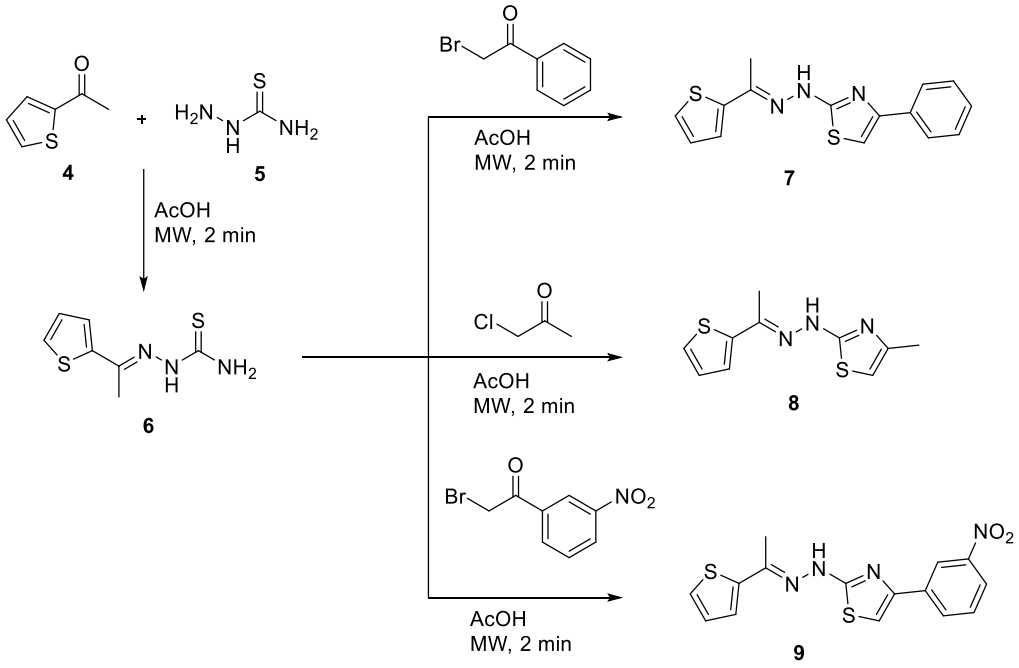

Scheme 5.2

Impressive one-pot thiazole synthesis was reported by Y. Liu *et al*[169]. New thiazole compounds **12** were produced by reacting carboxylic acid derivatives with β-azido disulphide ester in the presence of DBU and bromo trichloro methane **(Scheme 5.3)**.

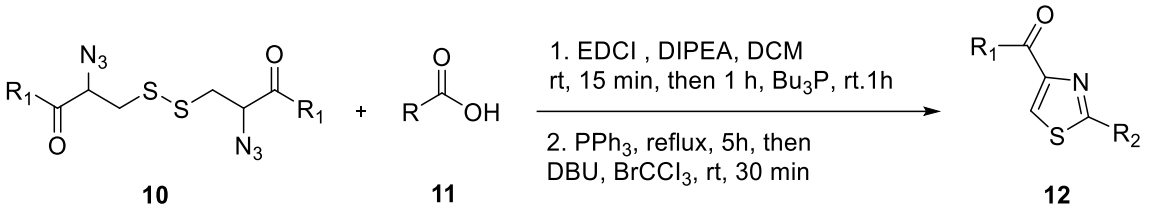

Scheme 5.3

The synthesis of thiazole derivatives **15** was reported by Z. Alsharif *et al*[70]. Using sodium acetate as a catalyst, 4-bromo-3-ethoxycrotonate and thiourea derivative **13** interacted in hexafluoro isopropanol to generate thiazole compounds 87 through refluxing for eight hours **(Scheme 5.4)**.

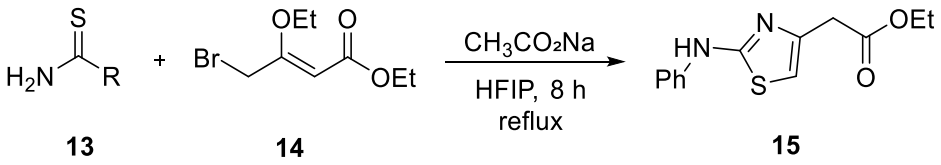

Scheme 5.4

Indole-thiazole compounds **20** were synthesised by A. Abdelhamid *et al*[171]. Indole **16** was the beginning point of the reaction, which added to thiosemicarbazide **17** to generate hydrazide compound **18**. A new thiazole compound **20** was created by the reaction of compound **18** with the two separate derivatives of phenacyl bromide and hydrazonoyl halide using method B. There are two reported ways of synthesizing thiazole-indole compounds **(Scheme 5.5)**.

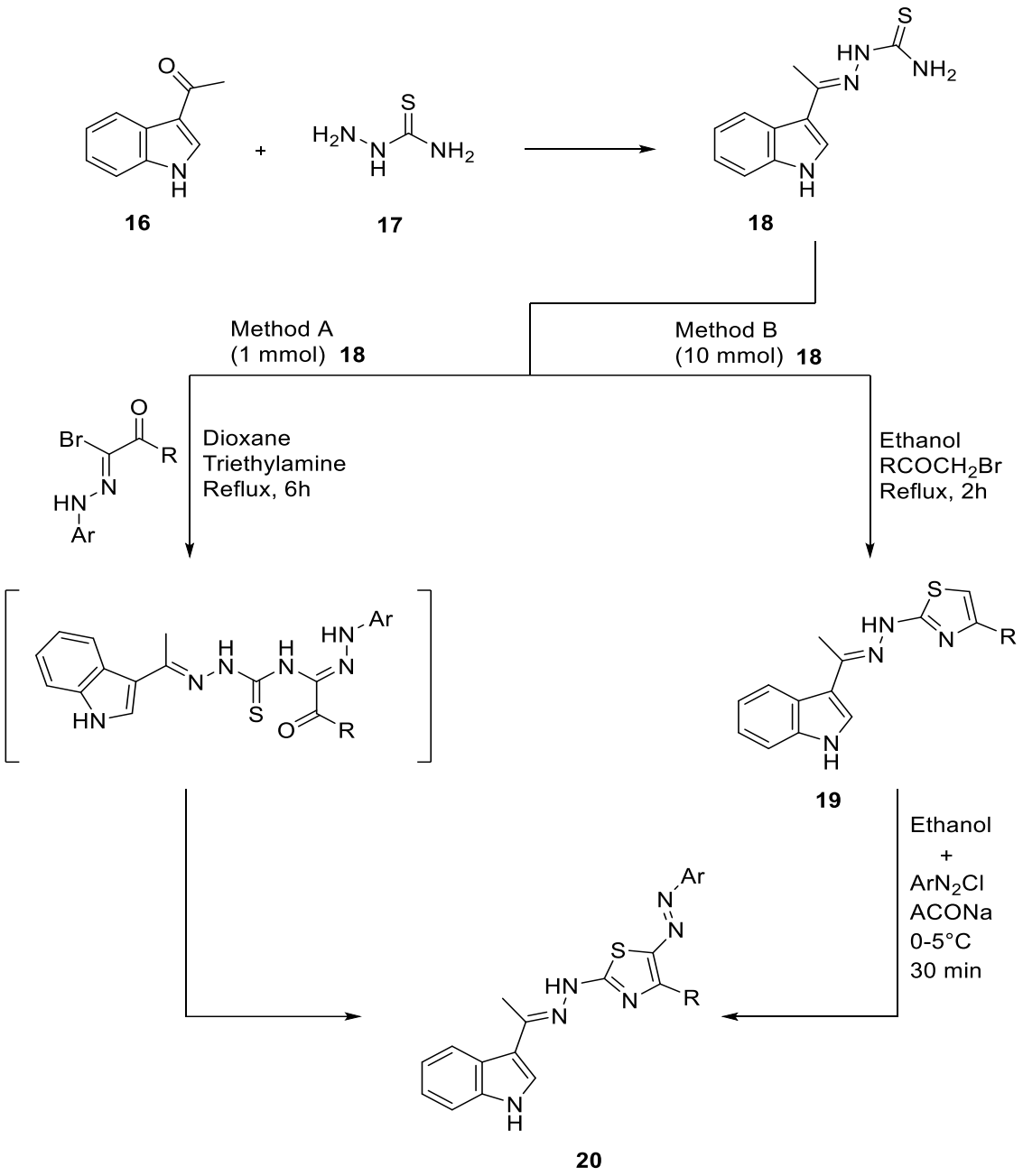
16
17
18
Method A
(1 mmol) 18
Method B
(10 mmol) 18
Dioxane
Triethylamine
Reflux, 6h
Ethanol
RCOCH2Br
Reflux, 2h
19
Ethanol
+
ArN2Cl
ACONa
0-5°C
30 min
20

Scheme 5.5

5.2. Results and Discussion

In our research, we explain the synthesis of various heterocyclic molecules in conjunction with the identification of a unique anti-malarial drug. Comprehensive information is given about 15 novel molecules, all of which have thiazolo as a key structural component. NMR, Mass spectroscopy and FTIR spectral data were used to analyze the spectrum profiles of compounds 5a–o. **Scheme 1** presents the synthesis of new and highly functionalized thiazoles derivative that contain amide, thiomethyl, ethyl ester, and ketene *N*, *S*-acetal linkages. Initially, easily accessible substances such as NBS, thiourea and acetoacetanilide were used to synthesize **3a-o**. Subsequently, compounds **3a–o** were reacted with **4a-o** in DMF with potassium carbonate as catalyst. This produced new and highly functionalized derivatives of thiazole **5a–o**, which are shown in **Scheme 1.**

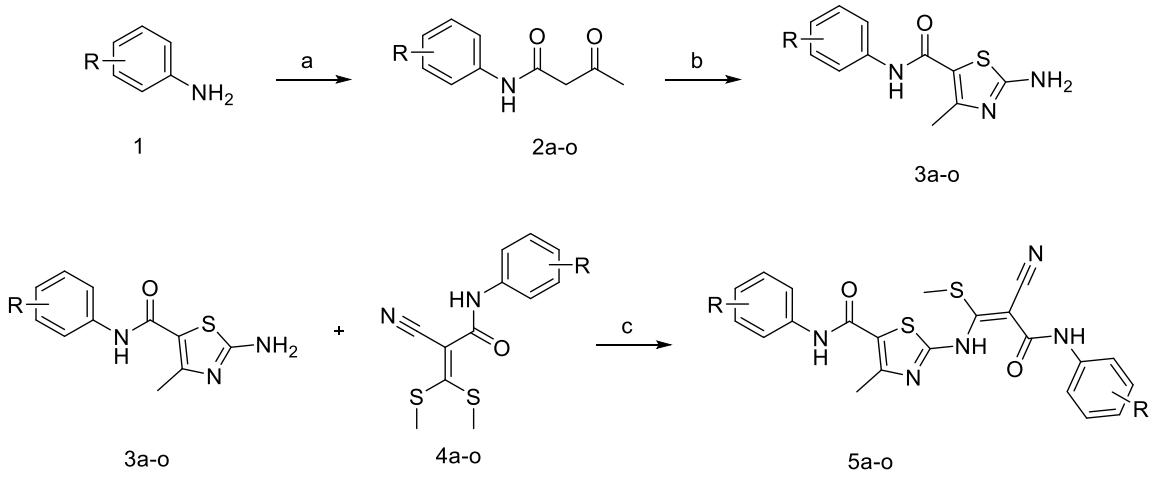

(a) Ethyl acetoacetate, KOH, Reflux, 24 hr (b) NBS, Thiourea, MeOH, Reflux, 4 hr (c) DMF ,K_2CO_3, rt, 1 hr

Scheme 1. Reagents and conditions.

The structural assignments for the recently synthesized compounds have been determined through careful examination of the elemental analyses and spectrum data. We provide detailed information on the elemental analysis as well as various types of physical characteristics of these new molecules. This provides an in-depth description of each substance's NMR, mass and FTIR spectra. Significantly, compounds show a characteristic proton singlet of the NH group between 9.54 and 13.31 ppm, while the aromatic region was seen between 7.11 and 7.67 ppm. Furthermore, the methyl group proton singlet is

detected between 2.26 and 2.51 ppm range. The molecular weight of each substance was confirmed by the presence of a molecular ion in its mass spectrum. In addition, the mass spectra show a molecular ion peak at 481, which is associated with the molecular formula $C_{23}H_{20}FN_5O_2S$.

Experimental conditions were optimized for the synthesis of compounds 5a–o by using a range of solvents, including acetone, methanol, tetrahydrofuran, ethanol, and IPA, as well as bases, including triethylamine and piperidine. This investigation revealed that using potassium carbonate together with DMF enhanced the reaction between 3a–o and 4a–o, generating a good yield of thiazole derivatives **5a–o**.

5.2.1. Optimizing reaction conditions

Table 1: Optimization of the reaction conditions

Entry	Solvent	Base [a]	Temp. (°C) [b]	Yield (%) [c]	Purification
1	No solvent	–	90	–	–
2	H_2O	–	rt	–	–
3	H_2O	K_2CO_3	rt	–	–
4	EtOH	Et_3N	rt	36	Yes
5	EtOH	K_2CO_3	rt	27	Yes
6	Acetone	Et_3N	rt	36	Yes
7	Acetone	K_2CO_3	rt	39	Yes
8	MeCN	Et_3N	rt	27	Yes
9	MeCN	K_2CO_3	rt	36	Yes
10	MeOH	Et_3N	rt	33	Yes
11	MeOH	K_2CO_3	rt	39	Yes
12	THF	Et_3N	rt	54	Yes
13	THF	K_2CO_3	rt	63	Yes
14	DMF	Et_3N	rt	83	Yes
15	DMF	K_2CO_3	rt	92	No

[a] Amount of base was 1 equivalent.
[b] Reaction time was 1 hr.
[c] Yield is given for isolated product without purification.

Initially, the reaction was first carried out at 90 °C without the use of a catalyst or solvent, but it was unable to produce any product. **(Table 1, entry 1)**. Following this, an experiment was conducted employing water as the solvent without a base at room temperature; however, once more, no product was obtained (entry 2). After that, an experiment was conducted with water as a solvent along with potassium carbonate at room temperature,

but no product was produced once more. (entry 3). In order to investigate various conditions, the reaction was carried out using ethanol as the solvent and triethylamine as the base. This resulted in a 36% product yield (entry 4), with a significantly lower 27% yield noted when potassium carbonate was used as the base (entry 5). A 36% product yield (entry 6) was obtained by changing the solvent to acetone with triethylamine as the base. This yield was further enhanced to 39% when potassium carbonate was used as the base (entry 7). After that, optimization was carried out with triethylamine as the base and acetonitrile as the solvent. This resulted in a 27% product yield (entry 8), while potassium carbonate as the base produced a 36% yield (entry 9). Utilizing triethylamine as catalyst and methanol as the solvent resulted in a 33% product yield (entry 10), whereas a 39% yield was achieved when potassium carbonate was used as the base (entry 11). Furthermore, an 54% product yield was obtained (entry 12) using tetrahydrofuran as the solvent and triethylamine as the base. This yield improved to 63% when potassium carbonate was used as the base (entry 13). Utilizing DMF in conjunction with triethylamine yielded an 83% yield (entry 14), while Employing potassium carbonate as the base and continuously stirring for an hour at room temperature resulted in an impressive 92% yield (entry 15). These results indicate that using potassium carbonate in conjunction with DMF produced thiazole compounds in satisfactory yields, suggesting faster reaction progress. Our approach was effectively applied to the synthesis of new thiazole derivatives by using the optimized reaction conditions, as the following table shows (**Table 2**).

5.2.2. Physicochemical Properties

Table 2: Physicochemical characteristics of the novel thiazole derivatives 5a-5o

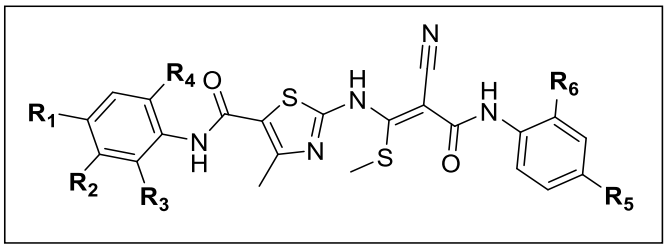

Entry	R_1	R_2	R_3	R_4	R_5	R_6	Yield (%)	Melting point (°C)
5a	CH_3	H	H	H	CH_3	CH_3	85	220–222
5b	H	Cl	H	H	CH_3	H	84	252–254
5c	F	H	H	H	CH_3	H	83	225–227
5d	Cl	H	H	H	CH_3	H	88	224–226
5e	Br	H	H	H	CH_3	H	81	272–274
5f	CH_3	H	H	CH_3	CH_3	H	87	210–212
5g	CH_3	H	H	H	CH_3	H	82	271–273
5h	F	H	H	H	F	H	89	235–237
5i	Cl	H	H	H	Br	H	82	221–223
5j	F	H	H	H	Br	H	85	258–260
5k	Br	H	H	H	Br	H	87	241–243
5l	Br	H	H	H	CH_3	CH_3	81	279–281
5m	H	H	OCH_3	H	CH_3	H	87	205–207
5n	CH_3	H	CH_3	H	CH_3	H	78	229–231
5o	H	H	CH_3	H	CH_3	H	85	253–225

Molecular docking was performed on newly synthesized thiazole compounds using Autodock to determine binding poses with affinity.

5.2.3. Molecular Docking with α-amylase

To determine the binding sites of a significant molecule, we use Autodock vina 1.5.7 to perform a molecular docking analysis on the Human pancreatic α-amylase. The Protein Data Bank provided the Human pancreatic α-amylase crystal structure, which has PDB id 2QV4. The co-crystallized ligand was redocked and superimposed with the ligand that was derived from the crystal structure in order to validate the molecular docking study. The reliability and accuracy of the molecular docking process were demonstrated by the root mean square deviation (RMSD), which was found to be 0.4 Ångstrom **(Figure 2).** Docking was applied to newly synthesized molecules, and the active site residues, binding energies and number of H-bonds are shown in **Table x.** The synthesized compounds showed a range of –8.5 to –9.8 kJ mol^{-1}, which was a favorable binding energy with the target. Compound 5n exhibited the most favorable docking score of -9.7 among all the molecules tested. Among the compounds that were studied, compound 5a showed docking score of -9.3, whereas compound 5b showed hydrogen bonding with ALA A:106, VAL A:107, resulting in a docking score of -9.2. The compound 5c and LYS A:200 created hydrogen bonds, resulting in a docking score of 9.3 **(Fig. 3)**. In addition, compound 5d established conventional hydrogen connections with THR A:163, resulting in a docking score of -9.1 **(Fig. 4)**. Compound 5f established two hydrogen bonds with the amino acids GLN A:63 and THR A:163, resulting in a docking score of -9.0. In addition, molecule 5g formed a standard hydrogen connection with THR A:163 and GLN A:63, resulting in a docking score of -9.4. While compound 5h show docking score -9.3, compound 5m formed hydrogen bonds with HIS A:305, resulting in a docking score of -8.5. Compound 5n demonstrated the highest docking score of –9.8, establishing conventional hydrogen bonds with THR A:163. Compound 5o achieved a docking score of –8.9 by forming conventional hydrogen bonds with HIS A:305.

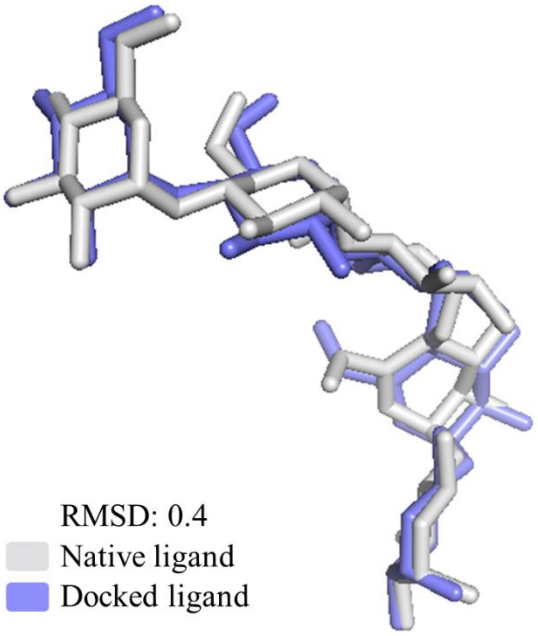

Fig 1. Validation of molecular docking protocol.

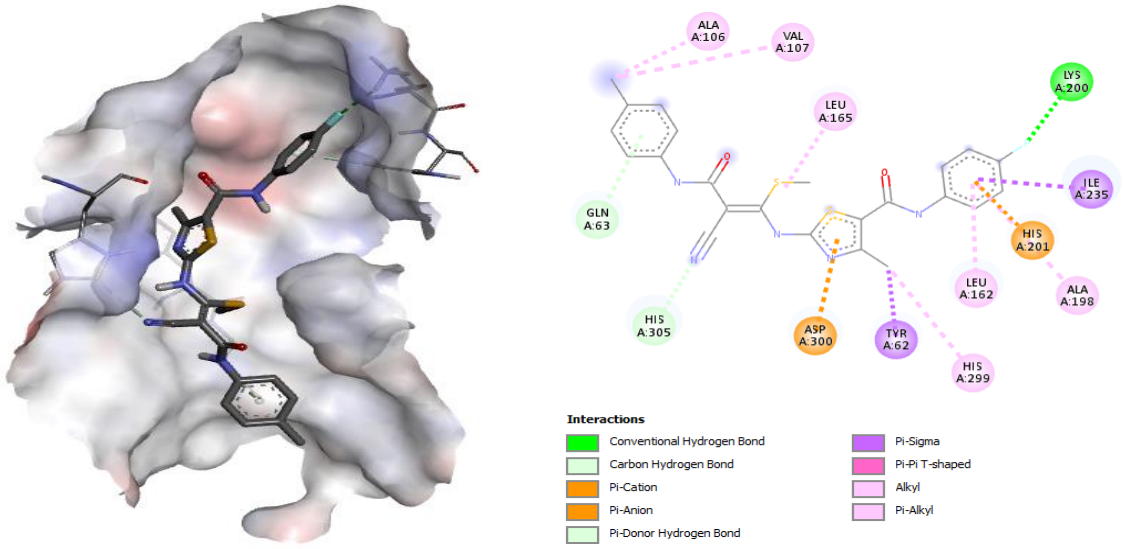

Fig 3: Docking pose of **5c** with human pancreatic α-amylase

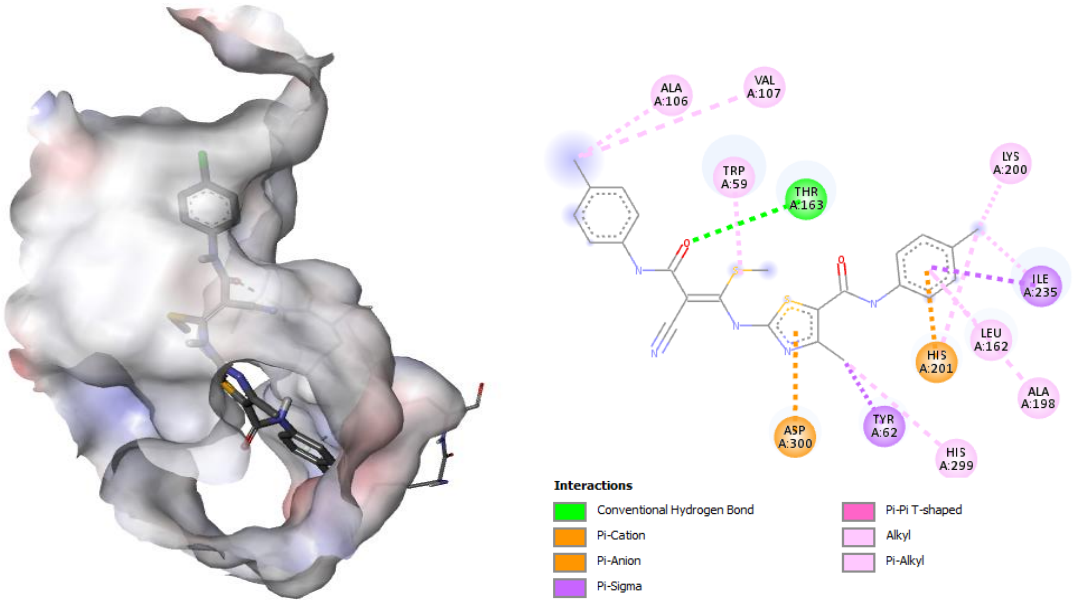

Fig 4: Docking pose of **5d** with human pancreatic α-amylase

5.2.4. *In vitro* α-amylase inhibition.

The Thiazole molecules **5a-o** were synthesized and analyzed for their in vitro activity against the human pancreatic α-amylase enzyme, with acarbose used as a reference compound following Mor's technique.

Table 3: Anti-diabatic activity

Compounds	**% Inhibition**				**IC_{50} (µg/mL)**
	12.5 (µg/mL)	**25 (µg/mL)**	**50 (µg/mL)**	**100 (µg/mL)**	
5a	23.08	37.61	50.89	78.15	40.05
5b	33.97	49.36	66.98	78.38	**25.08**
5c	51.33	65.45	71.96	85.63	**11.61**
5d	47.71	63.28	75.36	88.54	**14.05**
5e	41.17	55.82	77.61	91.41	**18.22**
5f	25.19	34.91	47.65	77.84	42.42
5g	28.53	56.84	75.67	91.98	**22.04**
5h	21.27	55.06	61.11	77.21	29.51
5i	32.28	47.03	60.45	72.14	30.03
5j	35.33	48.94	67.89	89.87	**23.49**
5k	23.71	57.16	63.57	79.19	**26.87**
5l	28.48	39.98	51.43	84.11	34.97
5m	15.19	37.98	43.06	64.78	55.86
5n	30.48	41.15	54.93	82.28	32.84
5o	17.43	33.76	49.43	65.51	51.72
Acarbose	38.43	50.22	64.33	90.42	28.02

The findings of the α-amylase inhibitory investigation are shown in **Table 3**, which shows that the investigated compounds 5a–o showed moderate to high levels of inhibition. Additionally, compounds 5c, 5d and 5e exhibited higher inhibition than acarbose at concentrations of 12.5 µg/mL, while compounds 5c, 5d, 5e, 5g, 5h and 5k displayed significant inhibition than acarbose at 25 µg/mL. compound 5b,5c,5d,5e,5g, and 5j

exhibited significant inhibition than acarbose at 100 µg/mL. On the other hand, some compounds demonstrated lesser inhibition than the control drug at various concentrations. Furthermore, **Table 3.** shows that compound 5b (IC_{50}=25.08 µg/mL), (IC_{50}= 11.61 µg/mL), 5d (IC_{50}=14.05 µg/mL), 5e (IC_{50}=18.22 µg/mL), 5g (IC_{50}=22.04 µg/mL) 5j (IC_{50}=23.49 µg/mL) and 5k (IC_{50}=26.87 µg/mL), among the synthesized compounds showed greater inhibition compared to acarbose (IC_{50}=28.02 µg/mL).

5.2.5. Prediction of the ADMET properties

Many possible drug candidates face failure in the drug development process because of their insufficient pharmacokinetics and physicochemical properties. By evaluating novel synthesized compounds using computational ADMET methods, it is possible to effectively address these limitations at the beginning of investigations.

Table 4: Physicochemical, Pharmacokinetic and Medicinal Chemistry Properties of the synthesized Molecule 5a-o

Physicochemical properties						**Pharmacokinetics**		**Medicinal chemistry**	
Compound	**HBA**	**HBD**	**TSPA**	**Log $P_{o/w}$**	**Log S**	**GIA**	**Log K_p**	**RoF (V)**	**SA**
4a	4	3	160.45	4.58	-9.26	Low	-4.96	Yes	4.20
4b	4	3	160.45	4.5	-9.73	Low	-4.68	Yes	3.96
4c	5	3	160.45	4.16	-8.61	Low	-5.35	Yes	3.96
4d	4	3	160.45	4.45	-9.16	Low	-5.07	Yes	3.95
4e	4	3	160.45	4.49	-9.22	Low	-5.3	No	3.99
4f	4	3	160.45	4.6	-9.83	Low	-4.57	Yes	4.19
4g	4	3	160.45	4.2	-8.88	Low	-5.14	Yes	4.09
4h	6	3	160.45	4.19	-8.34	Low	-5.56	Yes	3.9
4i	4	3	160.45	4.71	-9.49	Low	-5.24	No	3.89
4j	5	3	160.45	4.48	-8.95	Low	-5.51	No	3.91
4k	4	3	160.45	4.8	-9.56	Low	-5.46	No	3.93
4l	4	3	160.45	4.96	-10.17	Low	-4.73	No	4.10
4m	5	3	169.68	3.99	-9.24	Low	-5.12	Yes	4.05

4n	4	3	160.45	4.57	-9.26	Low	-4.96	Yes	4.19
4o	4	3	160.45	4.29	-9.46	Low	-4.74	Yes	4.09
Acarbose	19	14	321.17	-6.41	2.56	Low	-16.29	No	7.34

HBA: H-bond acceptor, HBD: H-bond donor, TPSA: Topological polar surface area, Log Po/w: Lipophilicity, Log S: Water Solubility, HIA: Human intestinal absorption, ROA: Rat Oral Acute Toxicity, RoF (V): Lipinski's Rule of five, SA: Synthetic accessibility.

The ADMET characteristics of the newly synthesized thiazolo compounds, including Synthetic Accessibility (SA), Lipophilicity (Log $P_{o/w}$), H-bond donor (HBD), Lipinski's Rule of five (RoF (V)), H-bond acceptor (HBA), gastrointestinal absorption (GIA), Water Solubility (Log S), Topological polar surface area (TSPA) and skin permeation (Log K_p) are outlined in **Table 4**. The results of the analysis demonstrated that the water solubility (Log S) of most synthetic compounds could be used to predict their bioavailability, with values for all thiazole derivatives ranging from –8.34 to –10.17 and the lipophilicity (Log Po/w) values were below 5 (ranging from 3.99 to 4.96). Synthesized compounds follow Lipinski's Rule of Five, except for 5e, 5i, 5j, 5k and 5l which has a molecular weight greater than 500. All the synthesized compounds were also assessed for complexity using the synthetic accessibility test. The results indicate that all thiazole derivatives achieved scores within the range of 3.90 to 4.20. The computational data are analyzed using Swiss ADME[98].

5.3. Conclusion

Design, synthesis, characterization and antidiabetic evaluation have been carried out on a novel series of thiazole 5a-o derivatives containing amide, nitrile, alkyl, and methylthio groups. The novel synthesized compound has been confirmed using NMR, mass spectroscopy and FTIR analysis. Several synthesized molecules demonstrated significant inhibitory activity against a-amylase. Additionally, this study highlights that molecule 5c (IC50= 11.61 µg/mL), 5d (IC50=14.05 µg/mL), 5e (IC50=18.22 µg/mL), 5g (IC50=22.04 µg/mL), and 5j (IC50=23.49 µg/mL) from the synthesized molecules exhibited higher inhibition levels compared to acarbose (IC50=23.62 µg/mL). A molecular docking analysis was also carried out on the human pancreatic α-amylase. Moreover, an assessment of their physicochemical and pharmacokinetic characteristics in relation to ADMET has been conducted.

5.4. Experimental Section

The melting points were measured using an electrothermal apparatus with open capillaries and were uncorrected. The Merck silica-gel 60 F254 precoated plates were used for thin-layer chromatography. Iodine vapor or UV light at 254 and 365 nm were used to visualize the molecules. By utilizing a Shimadzu FT-IR spectrometer, the ATR technique was used to record the IR spectra. A Bruker AVANCE III (400 MHz) spectrometer operated in DMSO-d6 conditions was utilized to get 1H spectra. Chemical shifts are expressed as δ ppm with respect to the internal standard, Tetramethylsilane (TMS). A Shimadzu GCMS QP2010 Ultra mass spectrometer was utilized in conjunction with a direct input probe to acquire mass spectra. The experiments were carried out in a standard atmospheric condition. All chemicals utilized in the experiments, sourced from CDH, Sigma Aldrich, Combi-Blocks, Molychem, SRL, Spectrochem, Merk and Loba.

- **General process for the synthesis of Acetoacetanilide (2a-i):**

A mixture of aromatic amines (1a-i) (10 mmol) and ethyl acetoacetate were refluxed for about 24 hours in toluene, together with a catalytic quantity of either sodium or potassium hydroxide lye (10%). When the reaction was finished, the solvent was vacuum-evaporated and crystallizing the residue from methanol to produce pure acetoacetanilide

- **General process for the synthesis of thiazoles (3a-o):**

N-bromo succinimide (30 mmol) was added to a stirred solution containing acetoacetanilide (20 mmol) (2a-o) in methanol and the mixture was agitated for 30 minutes at the ambient temperature. Thiourea (40 mmol) was gradually added to this reaction mixture, and it refluxed for four to five hours. The reaction's progress was monitored by TLC. After completion of reaction, the reaction mixture was cooled to room temperature and poured with stirring into ice-water, then neutralized with diluted hydrochloric acid.

- **General procedure for the synthesis of *(Z)*-2-((2-*cyano*-3-((4-arylphenyl)amino)-1-(methylthio)-3-oxoprop-1-en-1-yl)amino)-*N*-(4-arylphenyl)-4-methylthiazole-5-carboxamide (5a-o):**

A solution containing 3a-o (20 mmol) and 2a-o (20 mmol) in 20 mL of DMF, along with anhydrous potassium carbonate (20 mmol), was stirred at ambient temperature for 1 hours. The reaction's progress was monitored by TLC. After completion of reaction, the reaction mixture was poured into ice water with stirring, then neutralized with diluted hydrochloric acid. The solid obtained was filtered, washed with water, and then subjected to purification through recrystallization from dimethylformamide (DMF), resulting in the formation of crystals (5a-o).

***(Z)*-2-((2-*cyano*-3-((2,4-dimethylphenyl)amino)-1-(methylthio)-3-oxoprop-1-en-1-yl)amino)-4-methyl-*N*-(p-tolyl)thiazole-5-carboxamide (5a).**

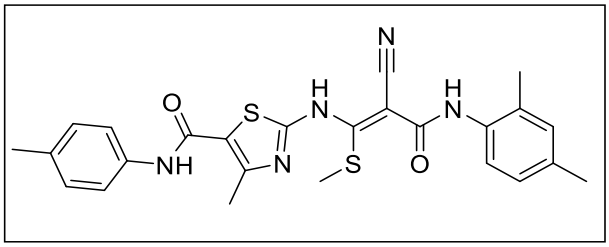

Yield 85%, mp 220–222 °C. IR spectrum, *v*, cm^{-1}: 3302.24 (-NH), 2214.35 (CN), 1674.27 (C=O), (CH_3). ^1H NMR spectrum, *δ*, ppm: Found, %: C, 61.14; H, 5.08; N, 14.33. $C_{25}H_{25}N_5O_2S_2$. Calculated, %: C, 61.08; H, 5.13; N, 14.25. *M* 491.

(*Z*)-*N*-(3-chlorophenyl)-2-((2-cyano-1-(methylthio)-3-oxo-3-(p-tolylamino)prop-1-en-1-yl)amino)-4-methylthiazole-5-carboxamide (5b).

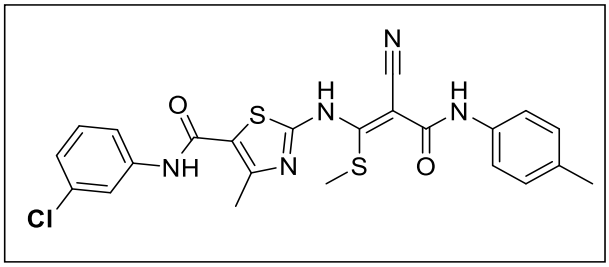

Yield 84%, mp 252–254 °C. IR spectrum, *v*, cm^{-1}: 3317.67 (-NH), 2206.64 (CN), 1643.41 (C=O), (CH_3). ^1H NMR spectrum, *δ*, ppm: Found, %: C 55.37; H, 3.98; N, 14.11. $C_{23}H_{20}ClN_5O_2S_2$. Calculated, %: C, 55.47; H, 4.05; N, 14.06 . *M* 498.

***(Z)*-2-((2-*cyano*-1-(methylthio)-3-oxo-3-(p-tolylamino)prop-1-en-1-yl)amino)-*N*-(4-fluorophenyl)-4-methylthiazole-5-carboxamide (5c).**

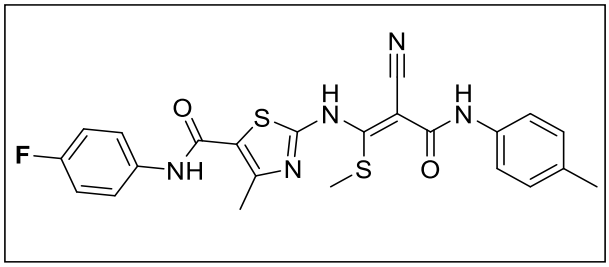

Yield 83%, mp 225–227 °C. IR spectrum, *v*, cm^{-1}: 3317.67 (-NH), 2198.92 (CN), 1635.69 (C=O), (CH_3). ^1H NMR spectrum, *δ*, ppm: 2.26 (s, 3H), 2.27 (s, 3H), 2.50 (s, 3H), 7.18-7.12 (m, 4H), 7.50 (d, *J* = 6.4 Hz, 2H), 7.64 (d, *J* = 7.6 Hz, 2H), 9.54 (s, 1H), 12.56 (s, 1H), 13.30 (s, 1H). Found, %: C, 57.41; H, 4.25; N, 14.43. $C_{23}H_{20}FN_5O_2S_2$. Calculated, %: C, 57.37; H, 4.19; N, 14.54. *M* 481.

(*Z*)-*N*-(4-chlorophenyl)-2-((2-cyano-1-(methylthio)-3-oxo-3-(p-tolylamino)prop-1-en-1-yl)amino)-4-methylthiazole-5-carboxamide (5d).

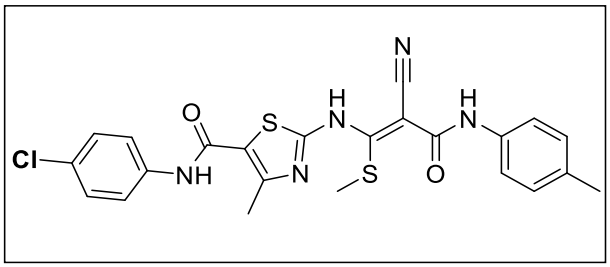

Yield 88%, mp 224–226 °C. IR spectrum, *v*, cm^{-1}: 3333.10 (-NH), 2203.08 (CN), 1633.33 (C=O). ^1H NMR spectrum, *δ*, ppm: 2.26 (s, 3H), 2.26 (s, 3H), 2.51 (s, 3H), 7.12 (d, *J* = 7.6 Hz ,2H), 7.39 (d, *J* = 7.6 Hz, 2H), 7.65-7.67 (m, 4H), 9.56 (s, 1H), 12.58 (s, 1H), 13.31 (s, 1H). Found, %: C, 55.53; H, 4.02; N, 14.17. $C_{23}H_{20}ClN_5O_2S_2$. Calculated, %: C, 55.47; H, 4.05; N, 14.06. *M* 498.

(*Z*)-*N*-(4-bromophenyl)-2-((2-cyano-1-(methylthio)-3-oxo-3-(p-tolylamino)prop-1-en-1-yl)amino)-4-methylthiazole-5-carboxamide (5e).

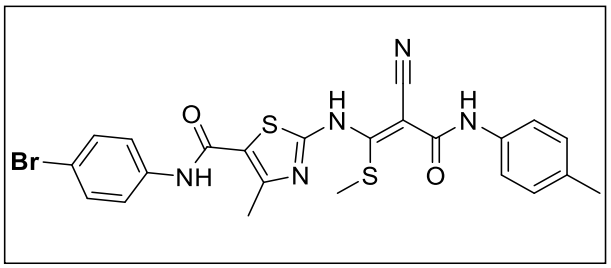

Yield 81%, mp 272–274 °C. IR spectrum, *v*, cm^{-1}: 3333.10 (-NH), 2198.92 (CN), 1643.41 (C=O). ^1H NMR spectrum, *δ*, ppm: 2.26 (s, 3H), 2.27 (s, 3H), 2.50 (s, 3H), 7.12 (d, *J* = 8 Hz, 2H), 7.503-7.536 (m, 4H), 7.61 (d, *J* = 9.2 Hz, 2H), 9.55 (s, 1H), 12.58 (s, 1H), 13.30 (s, 1H). Found, %: C, 50.89; H, 3.79; N, 12.93. $C_{23}H_{20}BrN_5O_2S_2$. Calculated, %: C, 50.93; H, 3.72; N, 12.91. *M* 542.

***(Z)-2-((2-cyano*-1-(methylthio)-3-oxo-3-(p-tolylamino)prop-1-en-1-yl)amino)-*N*-(2,6-dimethylphenyl)-4-methylthiazole-5-carboxamide (5f).**

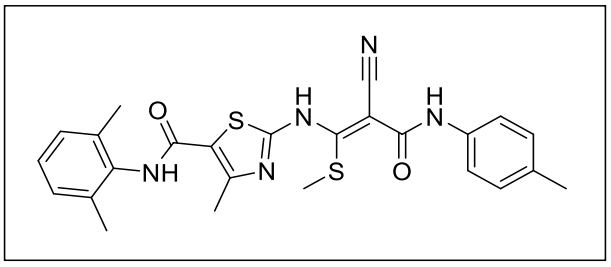

Yield 87%, mp 210–212 °C. IR spectrum, *v*, cm^{-1}: 3317.67 (-NH), 2214.35 (CN), 1705.13 (C=O), (CH_3). Found, %: C, 61.02; H, 5.21; N, 14.33. $C_{25}H_{25}N_5O_2S_2$. Calculated, %: C, 61.08; H, 5.13; N, 14.25. *M* 491.

***(Z)-2-((2-cyano*-1-(methylthio)-3-oxo-3-(p-tolylamino)prop-1-en-1-yl)amino)-4-methyl-*N*-(p-tolyl)thiazole-5-carboxamide (5g).**

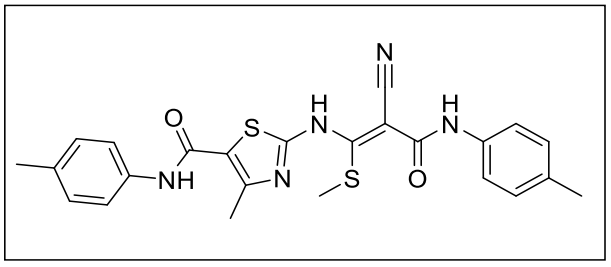

Yield 82%, mp 271–273 °C. IR spectrum, *v*, cm^{-1}: 3333.10 (-NH), 2206.64 (CN), 1728.28 (C=O). ^1H NMR spectrum, *δ*, ppm: 2.26 (s, 9H), 2.49 (s, 3H), 7.11-7.15 (m, 4H), 7.51-7.49

(m, 4H), 9.56 (s, 1H), 12.53 (s, 1H), 13.30 (s, 1H). Found, %: C, 60.31; H, 4.91; N, 14.57. $C_{24}H_{23}N_5O_2S_2$. Calculated, %: C, 60.36; H, 4.85; N, 14.66. *M* 477.

(*Z*)-2-((2-*cyano*-3-((4-fluorophenyl)amino)-1-(methylthio)-3-oxoprop-1-en-1-yl)amino)-*N*-(4-fluorophenyl)-4-methylthiazole-5-carboxamide (5h).

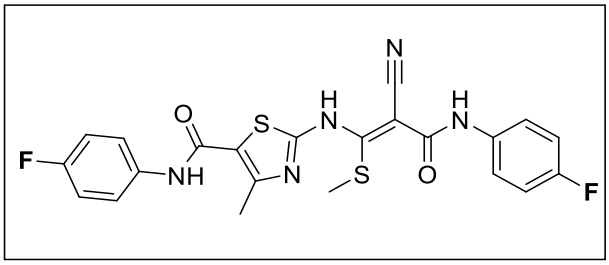

Yield 89%, mp 235–237 °C. IR spectrum, *v*, cm^{-1}: 3335.30 (-NH), 2198.92 (CN), 1638.78 (C=O). Found, %: C, 54.49; H, 3.47; N, 14.45. $C_{22}H_{17}F_2N_5O_2S_2$. Calculated, %: C, 54.42; H, 3.53; N, 14.42. *M* 485.

(*Z*)-2-((3-((4-bromophenyl)amino)-2-cyano-1-(methylthio)-3-oxoprop-1-en-1-yl)amino)-*N*-(4-chlorophenyl)-4-methylthiazole-5-carboxamide (5i).

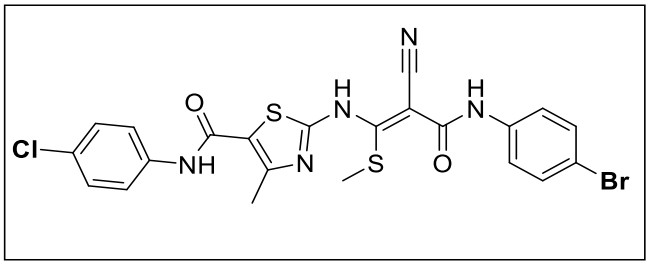

Yield 82%, mp 221–223 °C. IR spectrum, *v*, cm^{-1}: 3313.48 (-NH), 2209.77 (CN), 1644.91 (C=O). Found, %: C, 46.98; H, 2.98; N, 12.51. $C_{22}H_{17}BrClN_5O_2S_2$. Calculated, %: C, 46.94; H, 3.04; N, 12.44. *M* 562.

(*Z*)-2-((3-((4-bromophenyl)amino)-2-cyano-1-(methylthio)-3-oxoprop-1-en-1-yl)amino)-*N*-(4-fluorophenyl)-4-methylthiazole-5-carboxamide (5j).

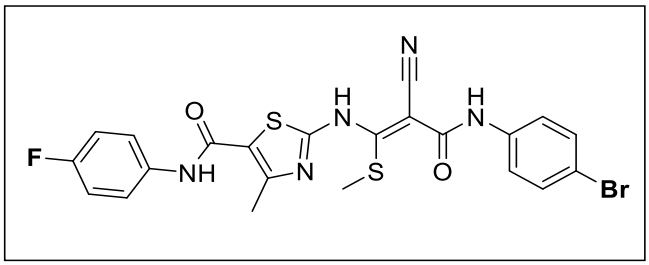

Yield 85%, mp 258–260 °C. IR spectrum, *v*, cm^{-1}: 332.31 (-NH), 2218.25 (CN), 1707.32 (C=O). Found, %: C 48.27; H 3.21; N 12.86. $C_{22}H_{17}BrFN_5O_2S_2$. Calculated, %: C, 48.36; H, 3.14; N, 12.82. *M* 546.

(*Z*)-*N*-(4-bromophenyl)-2-((3-((4-bromophenyl)amino)-2-cyano-1-(methylthio)-3-oxoprop-1-en-1-yl)amino)-4-methylthiazole-5-carboxamide (5k).

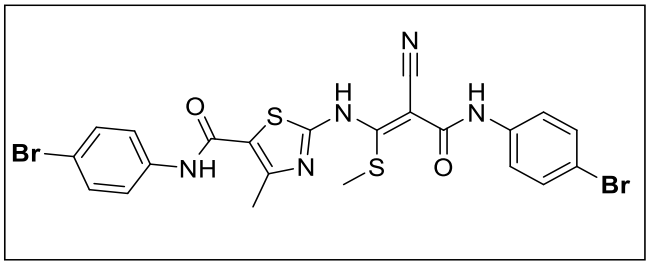

Yield 87%, mp 241–243 °C. IR spectrum, *v*, cm^{-1}: 3336.21 (-NH), 2195.08 (CN), 1646.91 (C=O). Found, %: C, 43.55; H, 2.77; N, 11.61. $C_{22}H_{17}Br_2N_5O_2S_2$. Calculated, %: C, 43.51; H, 2.82; N, 11.53. *M* 607.

(*Z*)-*N*-(4-bromophenyl)-2-((2-cyano-3-((2,4-dimethylphenyl)amino)-1-(methylthio)-3-oxoprop-1-en-1-yl)amino)-4-methylthiazole-5-carboxamide (5l).

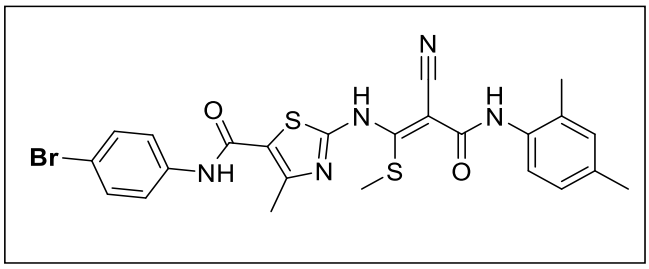

Yield 81%, mp 279–281 °C. IR spectrum, *v*, cm^{-1}: 3317.67 (-NH), 2206.64 (CN), 1643.41 (C=O). Found, %: C, 51.91; H, 3.88; N, 12.65. $C_{24}H_{22}BrN_5O_2S_2$. Calculated, %: C, 51.80; H, 3.98; N, 12.58. *M* 556.

***(Z)-2-((2-cyano*-1-(methylthio)-3-oxo-3-(p-tolylamino)prop-1-en-1-yl)amino)-N-(2-methoxyphenyl)-4-methylthiazole-5-carboxamide (5m).**

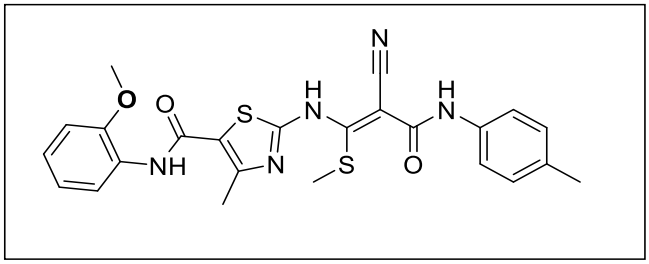

Yield 87, mp 205–207 °C. IR spectrum, *v*, cm^{-1}: 3319.64 (-NH), 2209.87 (CN), 1641.91 (C=O). Found, %: C, 58.31; H, 4.72; N, 14.23. $C_{24}H_{23}N_5O_3S_2$. Calculated, %: C, 58.40; H, 4.70; N, 14.19 . *M* 493.

***(Z)-2-((2-cyano*-1-(methylthio)-3-oxo-3-(p-tolylamino)prop-1-en-1-yl)amino)-*N*-(2,4-dimethylphenyl)-4-methylthiazole-5-carboxamide (5n).**

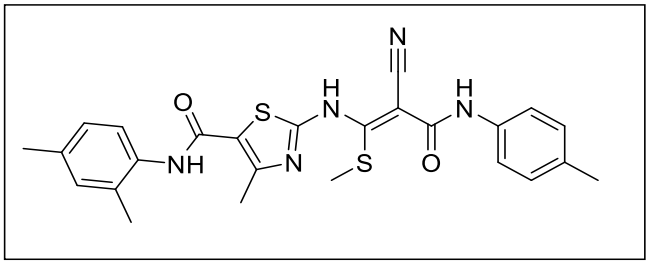

Yield 78, mp 229–231 °C. IR spectrum, *v*, cm^{-1}: 3319.34 (-NH), 2216.91 (CN), 1707.68 (C=O). Found, %: C 61.14; H, 5.21; N, 14.18. $C_{25}H_{25}N_5O_2S_2$. Calculated, %: C, 61.08; H, 5.13; N, 14.25. *M* 491.

***(Z)-2-((2-cyano*-1-(methylthio)-3-oxo-3-(p-tolylamino)prop-1-en-1-yl)amino)-4-methyl-*N*-(o-tolyl)thiazole-5-carboxamide (5o).**

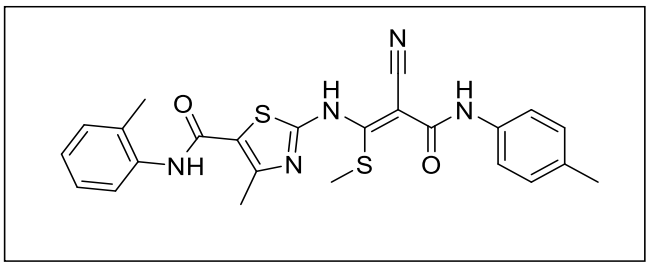

Yield 85, mp 253–22 °C. IR spectrum, *v*, cm^{-1}: 3333.10 (-NH), 2203.16 (CN), 1634.91 (C=O), (CH_3). Found, %: C, 60.28; H, 4.91; N, 14.59. $C_{24}H_{23}N_5O_2S_2$. Calculated, %: C, 60.36; H, 4.85; N, 14.66. *M* 477.

5.4.1. Experimental protocol of molecular docking study

ChemSketch 2022.2.3 was used to create the ligand structures. Additionally, docking investigations were conducted using Autodock Vina 1.5.7[98]. Crystallographic information for the PfDHFR enzyme, which the PDB database designated as 3QGT, was referenced. In order to assure accurate molecular structure optimization as well as improve the reliability and accuracy of our computational research, Avogadro software was carefully used for energy minimization, applying the MMFF94 force field. All ligands had been eliminated from the structural receptor before docking by removing heteroatoms. When making proteins, water molecules were eliminated and polar hydrogens and Kollman charges were added. The grid point spacing was set at 0.375 angstroms, exhaustiveness value at 8, and the x, y, and z axes' grid box size were set at 40 Å each, with the centers at coordinates 12.384745, 48.136073, and 26.209218, respectively. Using Discovery Studio v21.1.0.20298, the likely binding mode was identified[172].

5.4.2. *In vitro* α-amylase inhibition

The evaluation of α-amylase inhibition activity in a controlled laboratory environment was carried out using Mor's technique[173], and the reference compound for comparison was acarbose. A variety of concentrations, including 12.5, 25, 50, and 100 mg/mL, were achieved by dissolving the molecule 4a-t in 5 mL of DMSO at ambient temperature. To prepare the substrate solution, 500 mg of starch was dissolved in a 25 mL solution of 0.4 M NaOH at 100°C for 5 minutes. Once cooled to room temperature, the pH was adjusted to 7 using a 2 M HCl solution. The final volume was then reached by adding 100 mL of water. The samples (20L) and substrate (40L) were combined in micro-plates and incubated at a temperature of 37 °C for a duration of three minutes. Subsequently, 20 mL of a solution containing α-amylase at a concentration of 50 µg/mL was introduced into each well, and the samples were allowed to incubate for 15 minutes. In order to cease the reaction, 0.1 M HCl (80 mL) was introduced. The reaction mass was supplemented with a 200 mL solution of 1 mM iodine, and the absorbance was then measured at 650 nm using an Elisa micro-plate reader. The percentage inhibition showed the activity of α -amylase inhibition.

$$\% \text{ inhibition} = \{1-(Abs2-Abs1)/(Abs4-Abs3) \times 100\}$$

5.5. Spectral Data

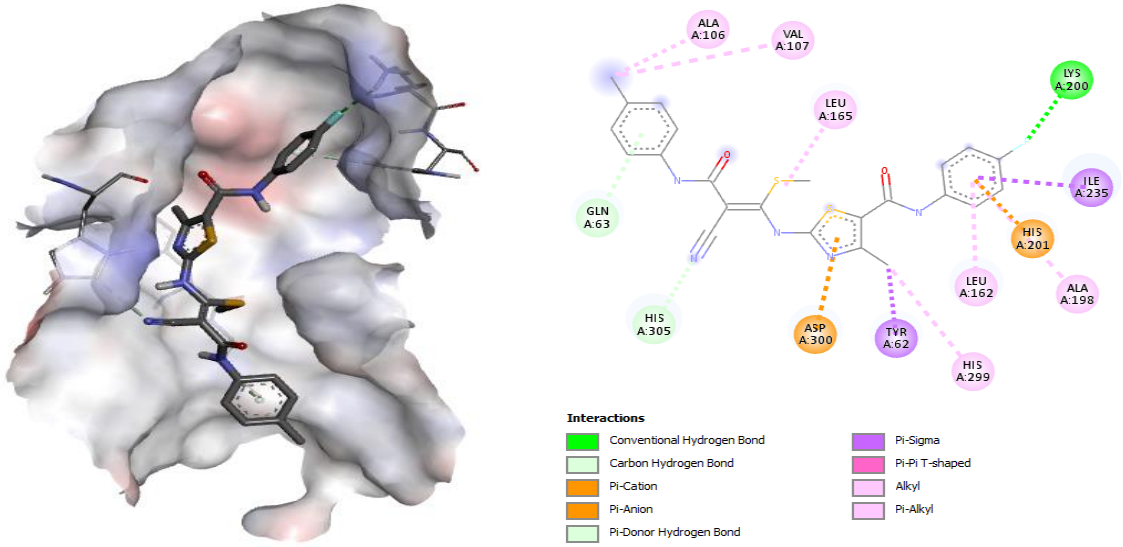

Fig. 1: Docking pose of **5c** with human pancreatic α-amylase

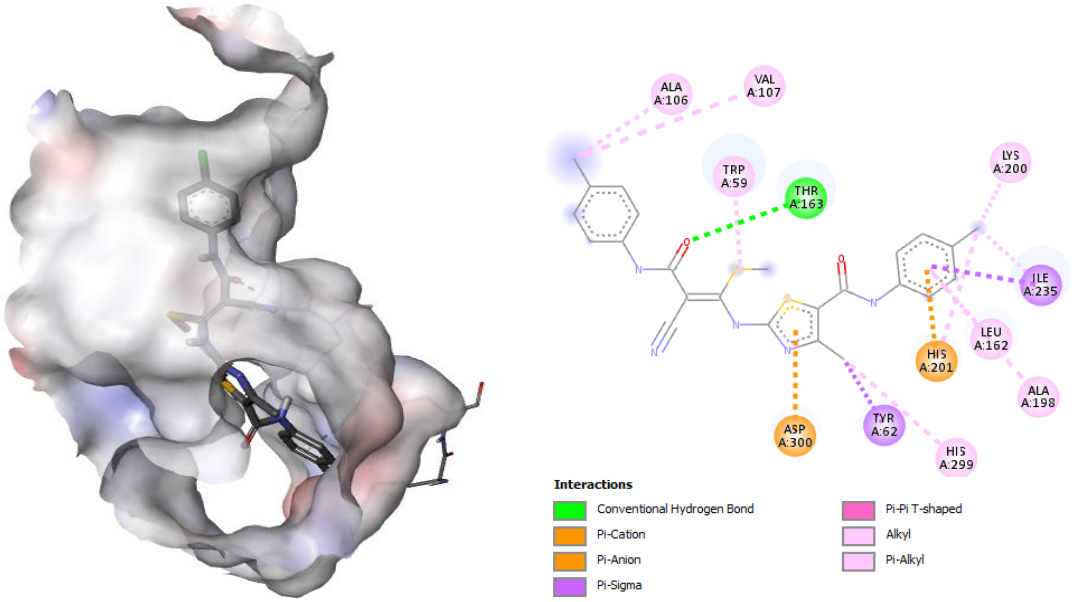

Fig. 2: Docking pose of **5d** with human pancreatic α-amylase

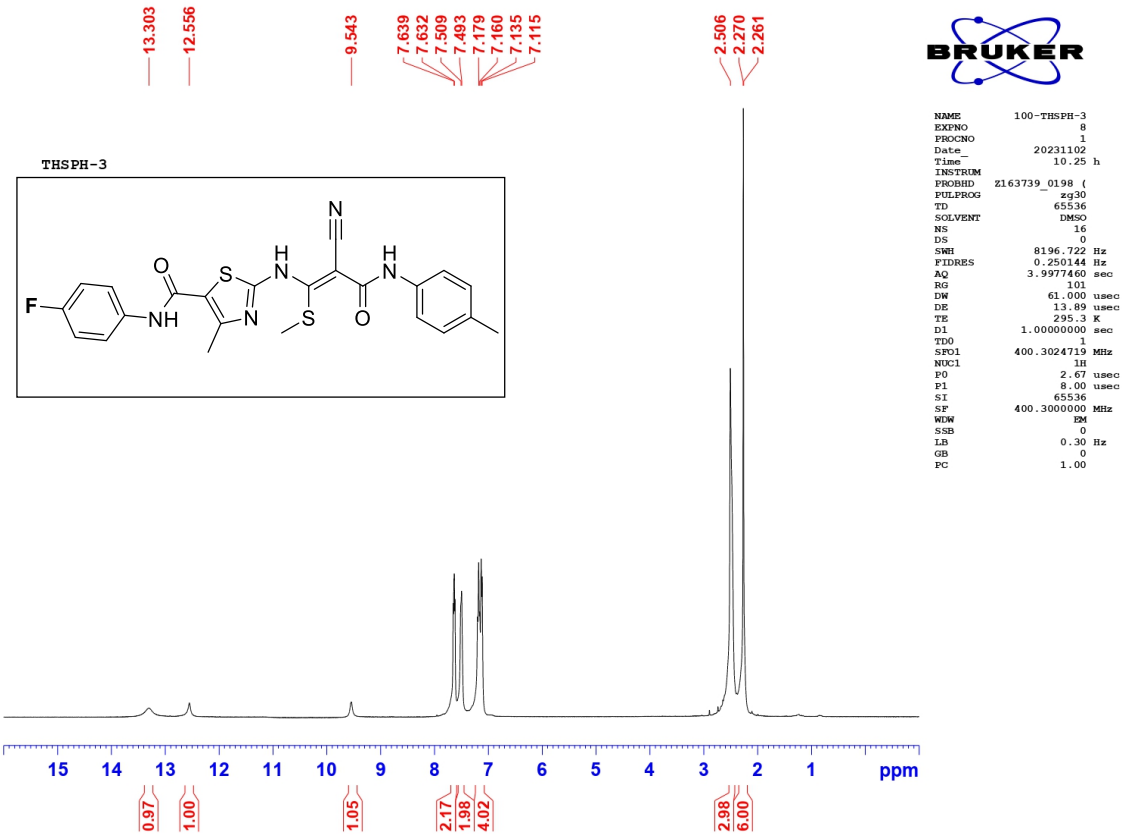

Fig. 3: Representative ^{1}H NMR spectrum of compound **THSPH-3**

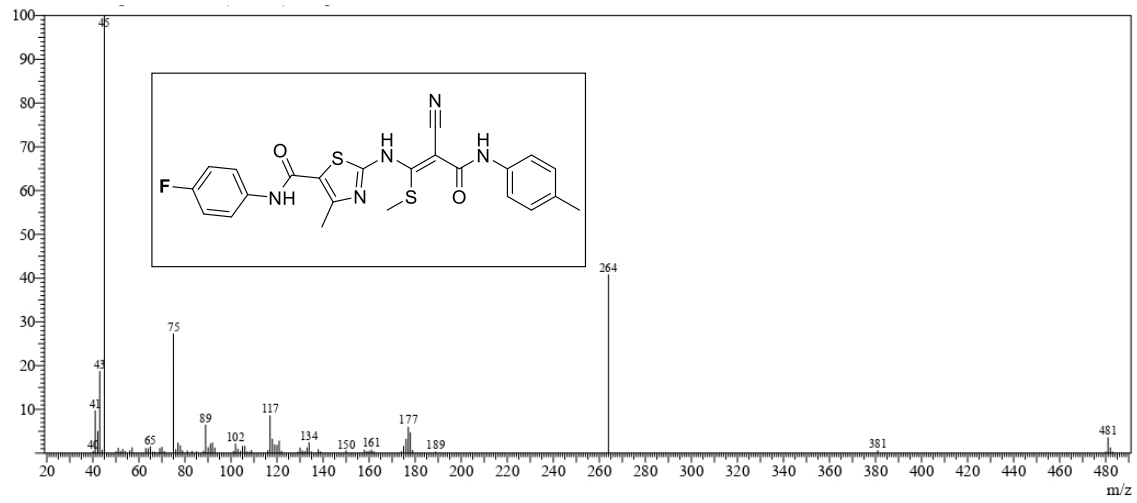

Fig. 4: Representative mass spectrum of compound **THSPH-3**

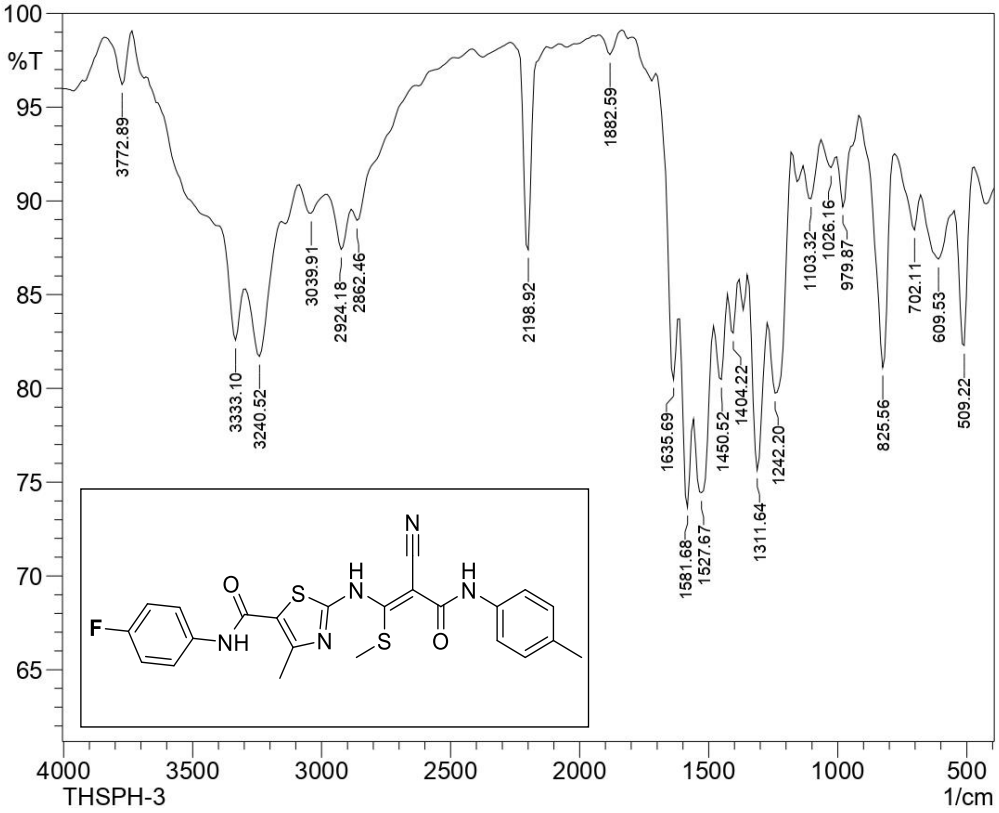

Fig. 5: Representative IR spectrum of compound **THSPH-3**

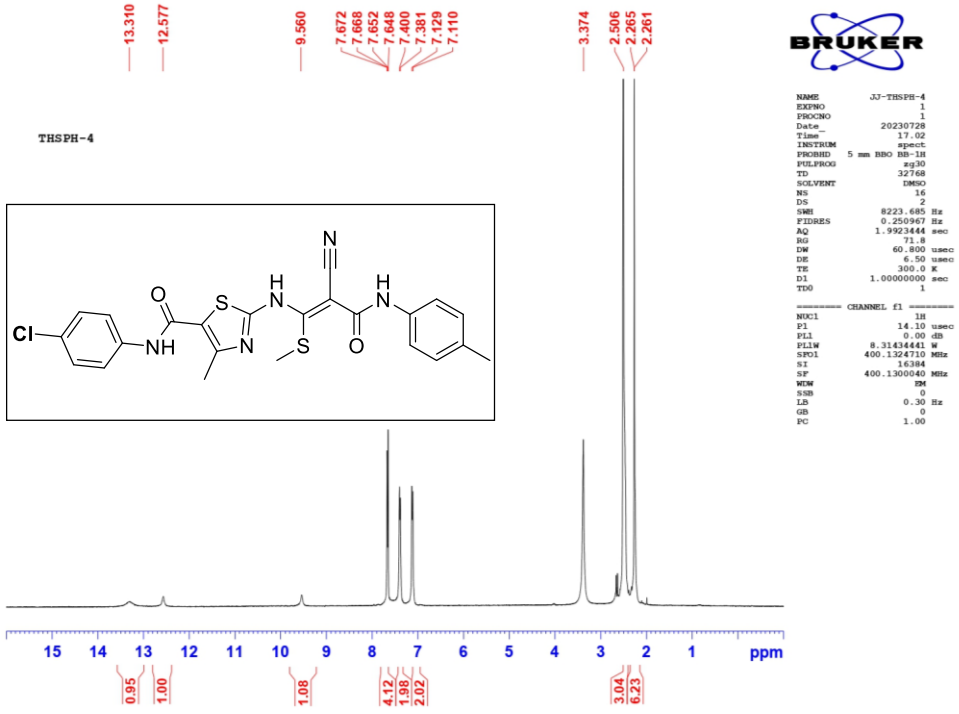

Fig. 6: Representative ^{1}H NMR spectrum of compound **THSPH-4**

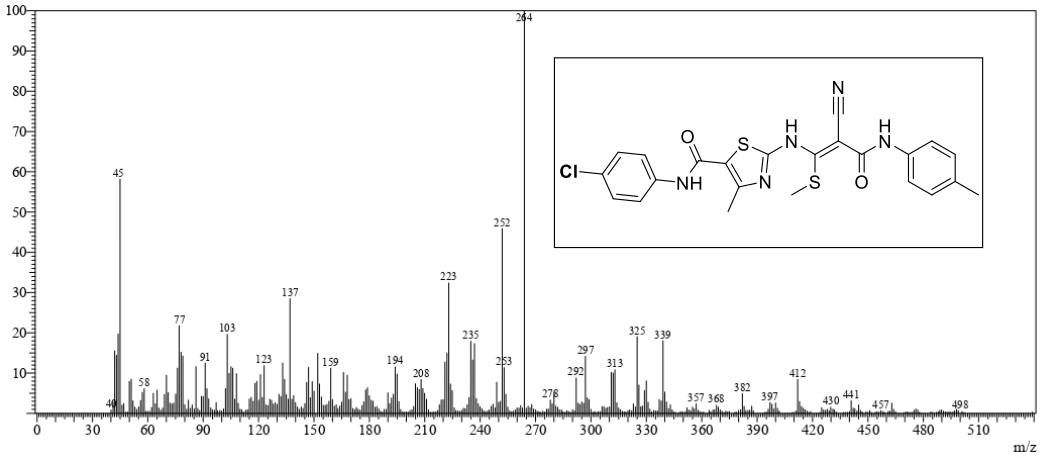

Fig. 7: Representative mass spectrum of compound **THSPH-4**

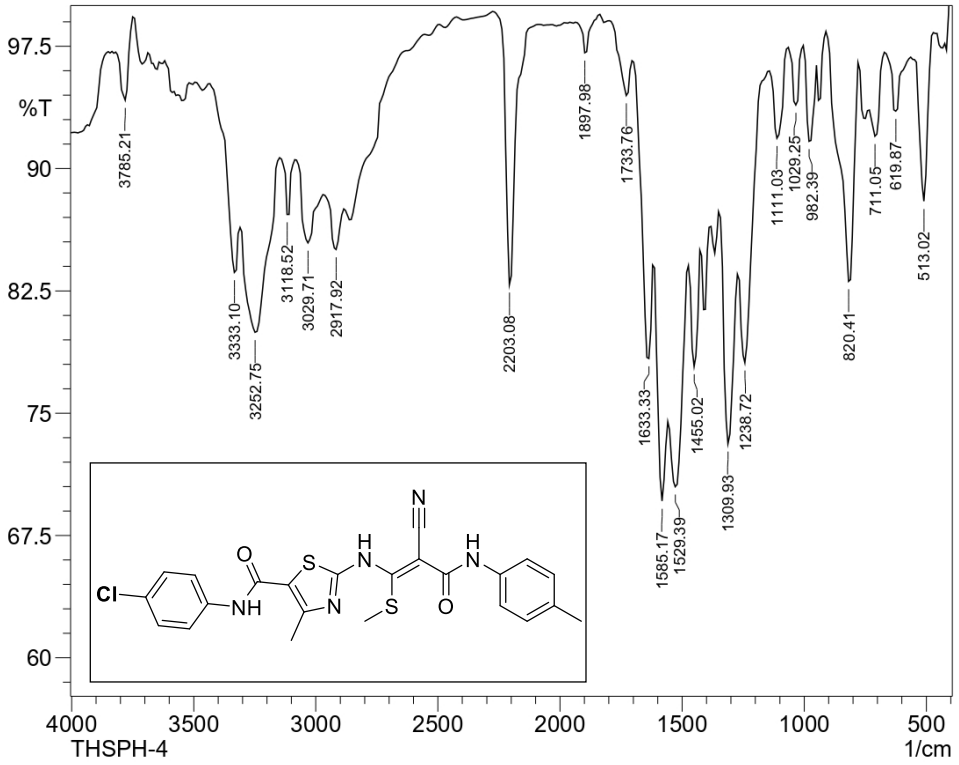

Fig. 8: Representative IR spectrum of compound **THSPH-4**

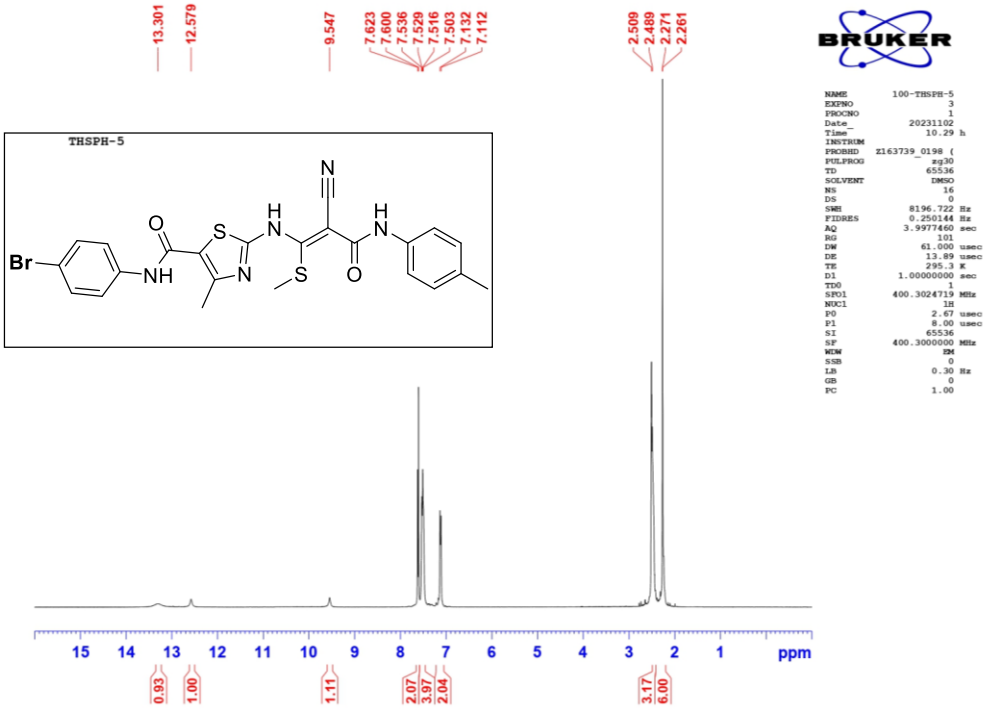

Fig. 9: Representative ^{1}H NMR spectrum of compound **THSPH-5**

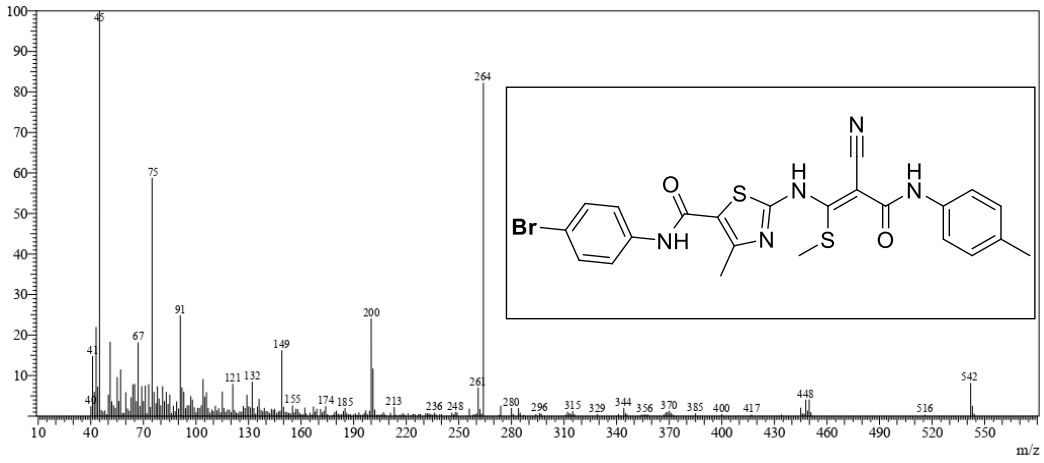

Fig. 10: Representative mass spectrum of compound **THSPH-5**

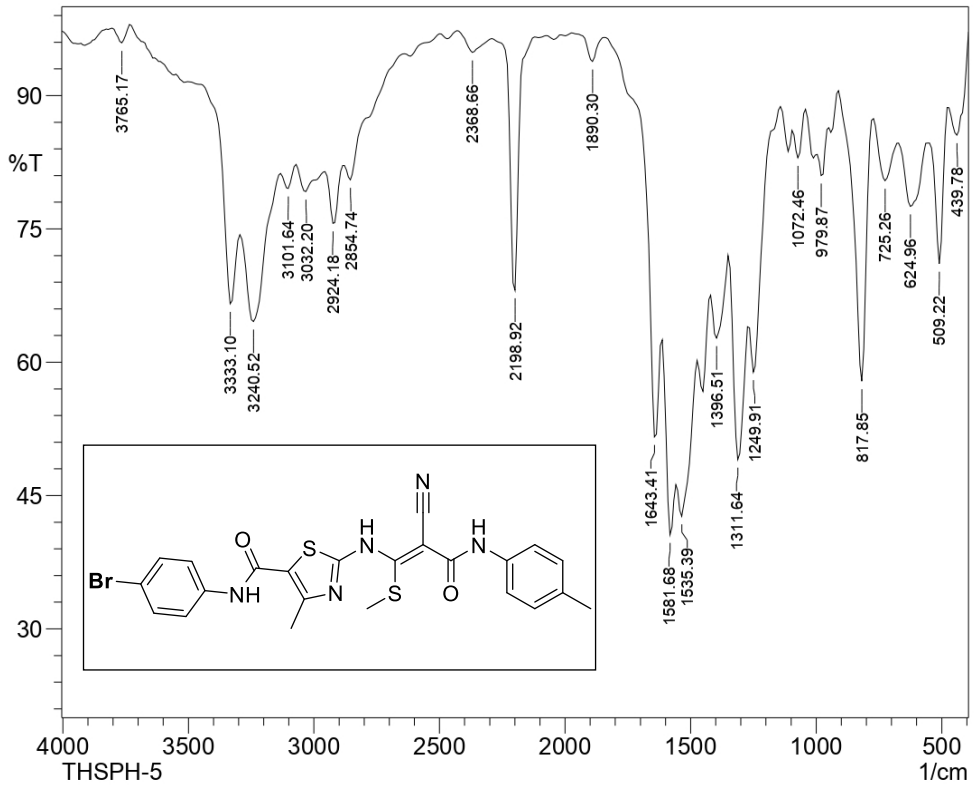

Fig. 11: Representative IR spectrum of compound **THSPH-5**

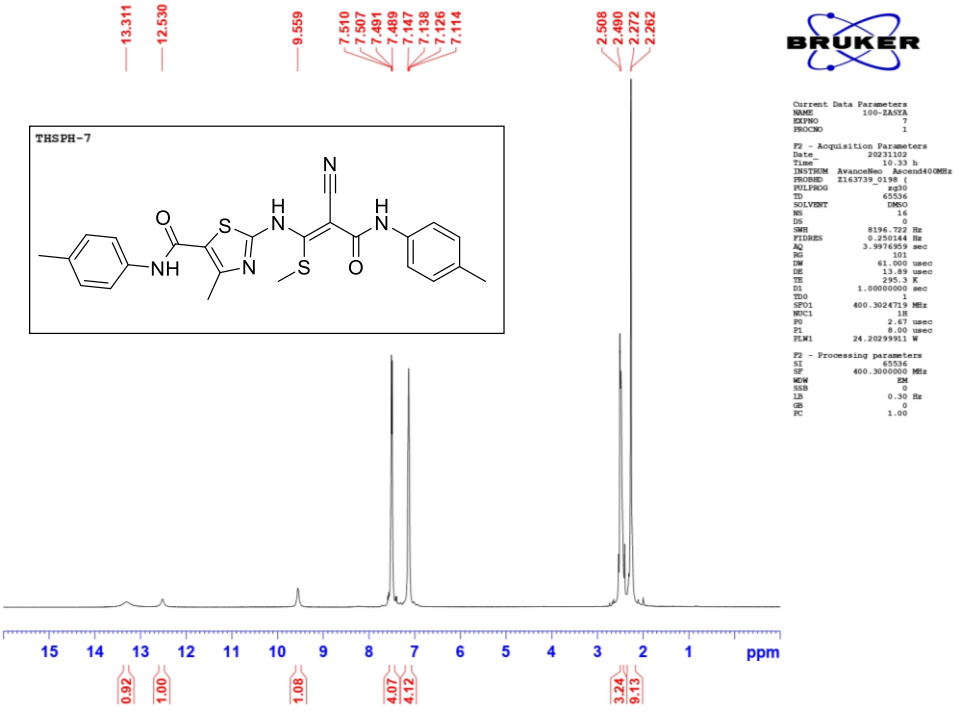

Fig. 12: Representative ^{1}H NMR spectrum of compound **THSPH-7**

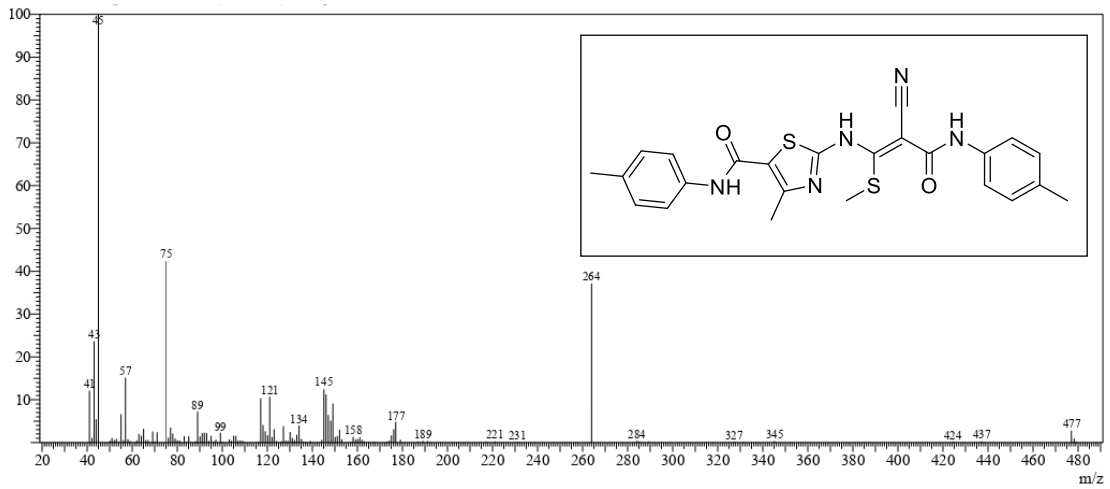

Fig. 13: Representative mass spectrum of compound **THSPH-7**

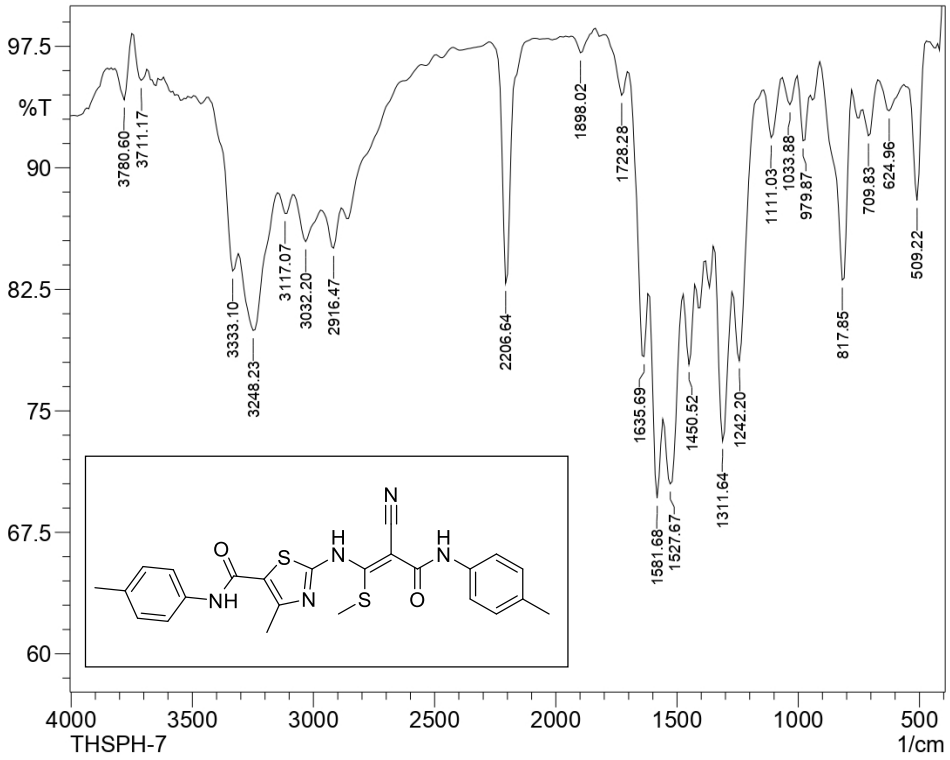

Fig. 14: Representative IR spectrum of compound **THSPH-7**

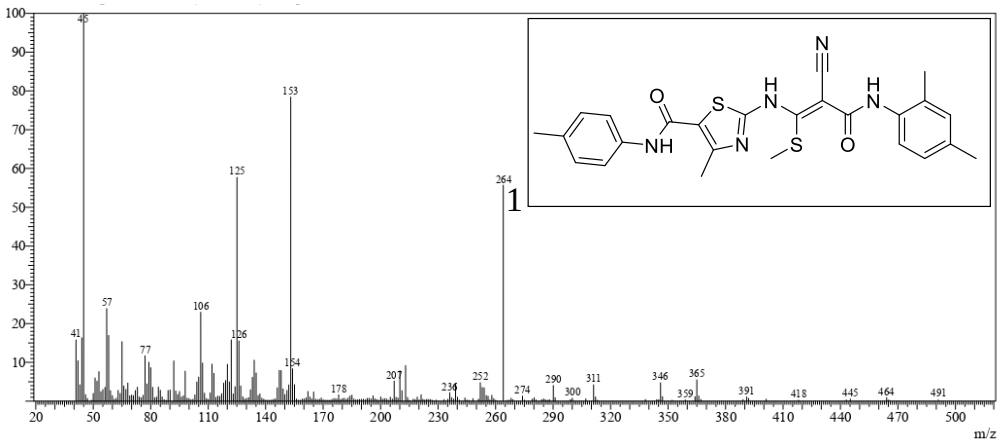

Fig. 15: Representative mass spectrum of compound **THSPH-1**

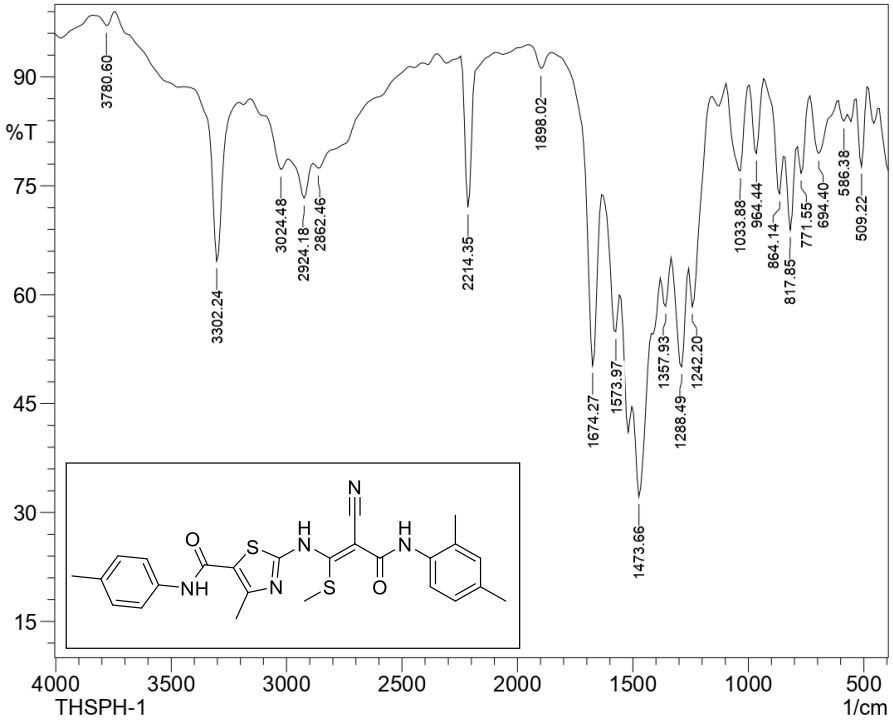

Fig. 16: Representative IR spectrum of compound **THSPH-1**

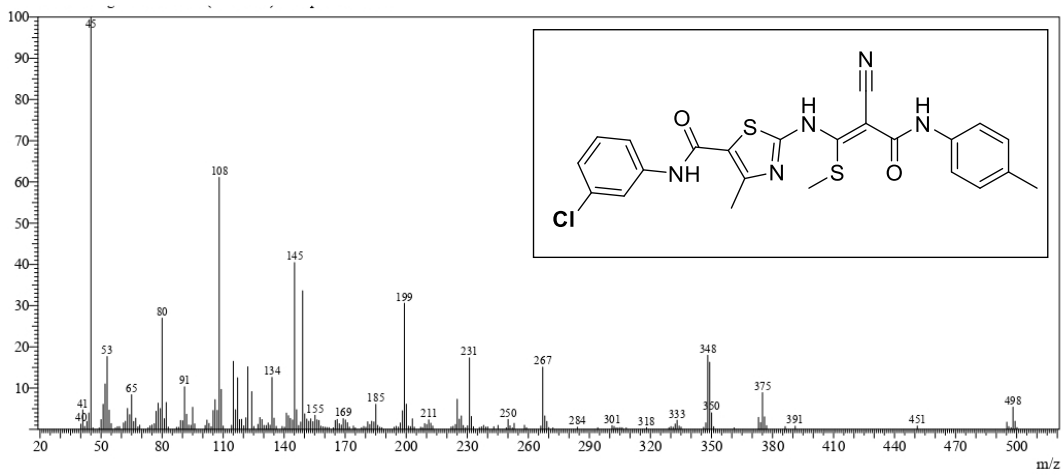

Fig. 17: Representative mass spectrum of compound **THSPH-2**

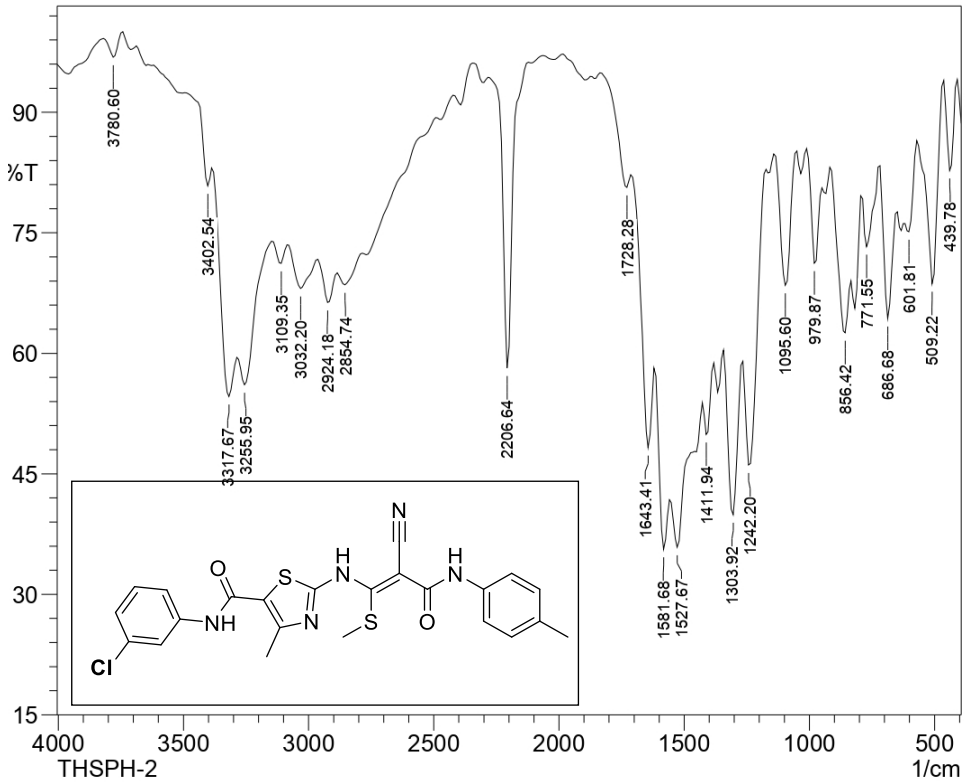

Fig. 18: Representative IR spectrum of compound **THSPH-2**

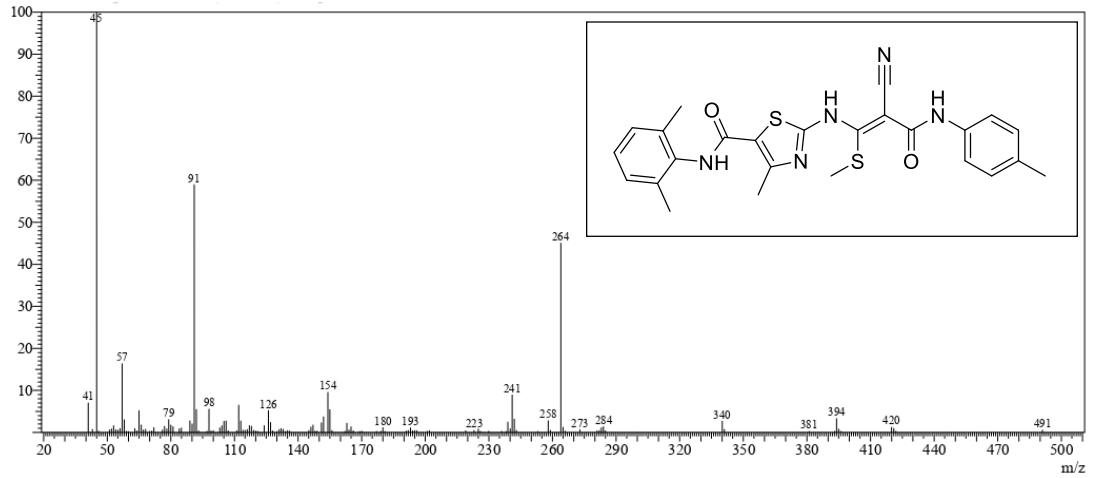

Fig. 19: Representative mass spectrum of compound **THSPH-6**

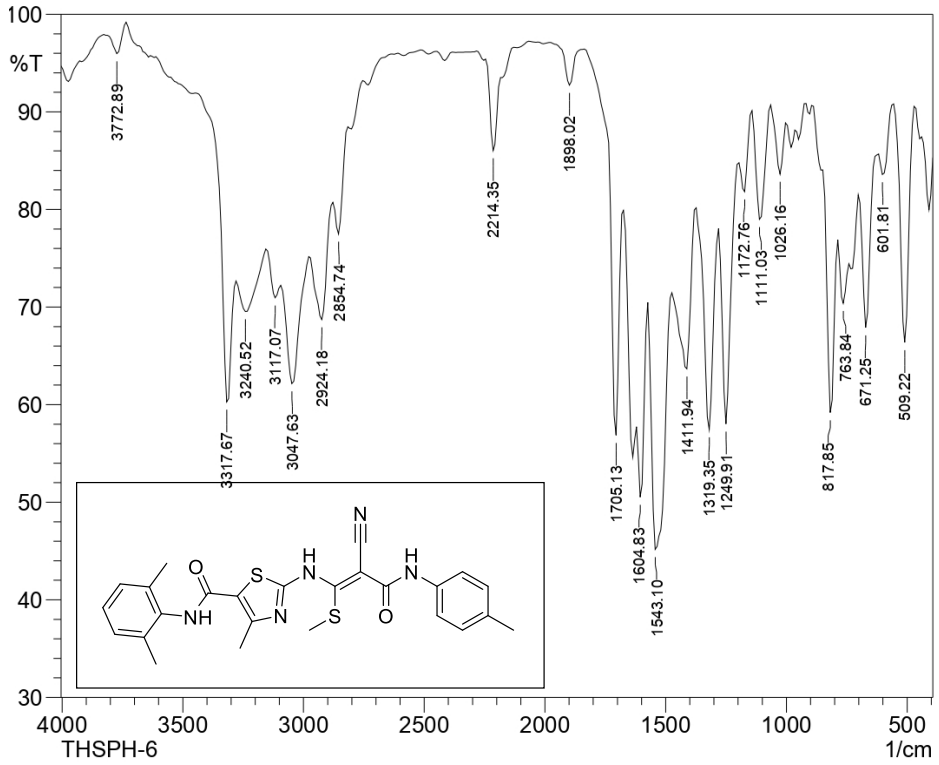

Fig. 20: Representative IR spectrum of compound **THSPH-6**

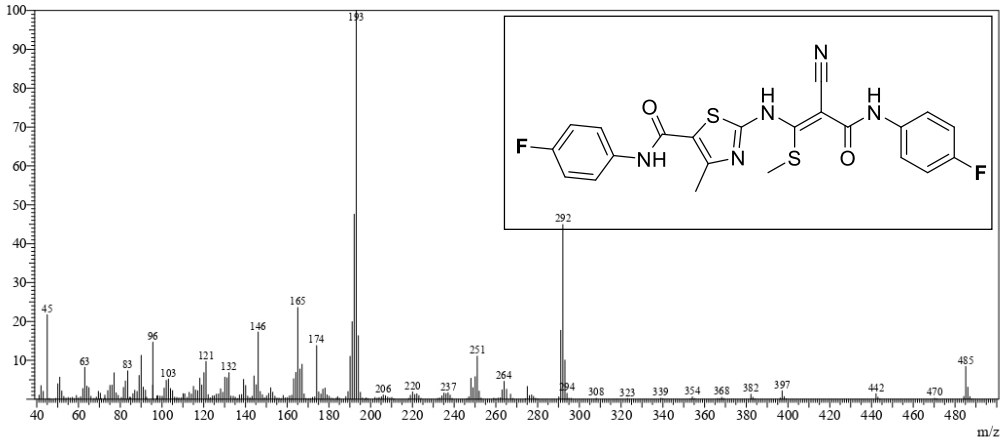

Fig. 21: Representative mass spectrum of compound **THSPH-8**

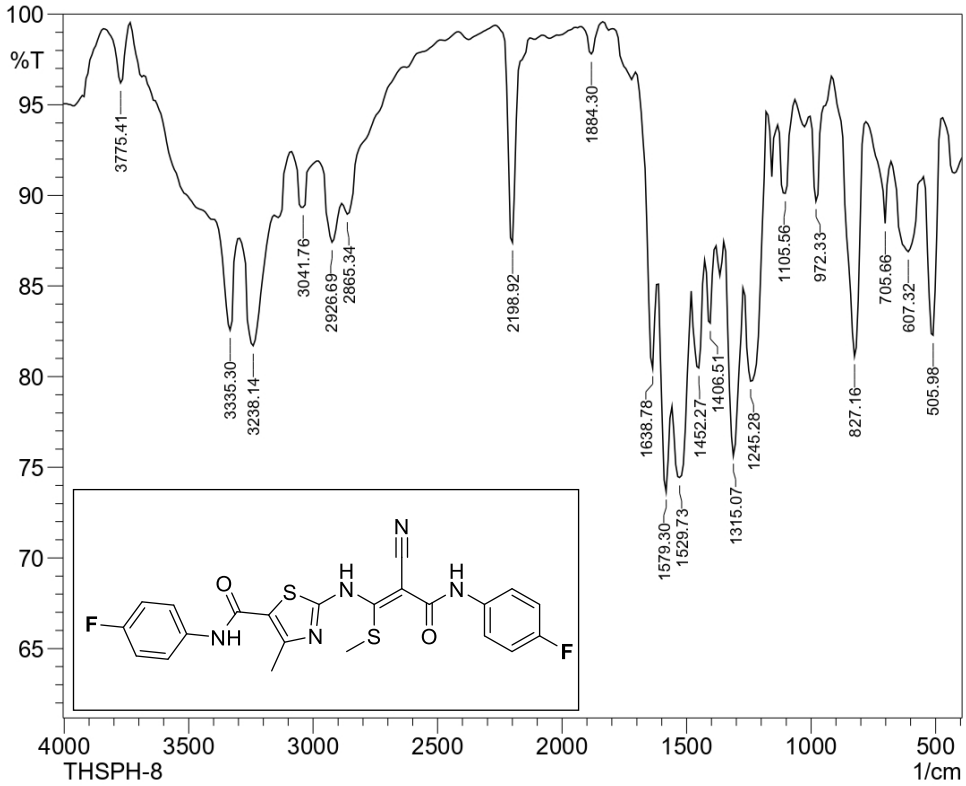

Fig. 22: Representative IR spectrum of compound **THSPH-8**

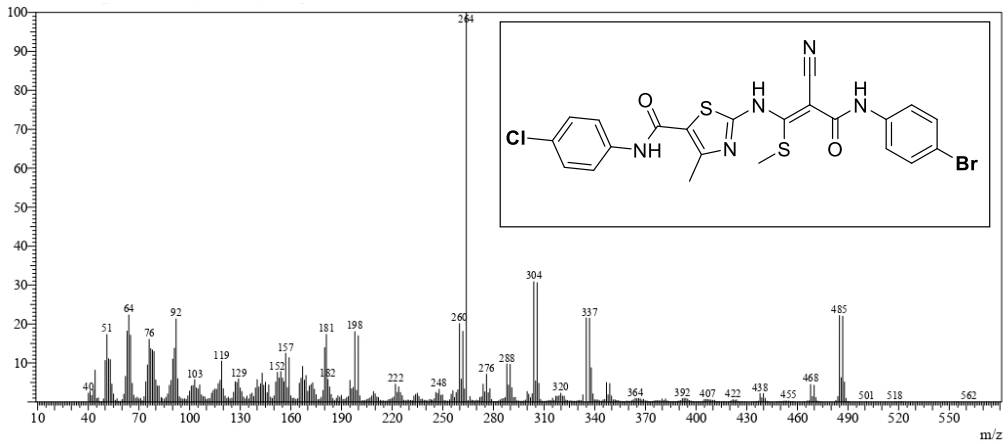

Fig. 23: Representative mass spectrum of compound **THSPH-9**

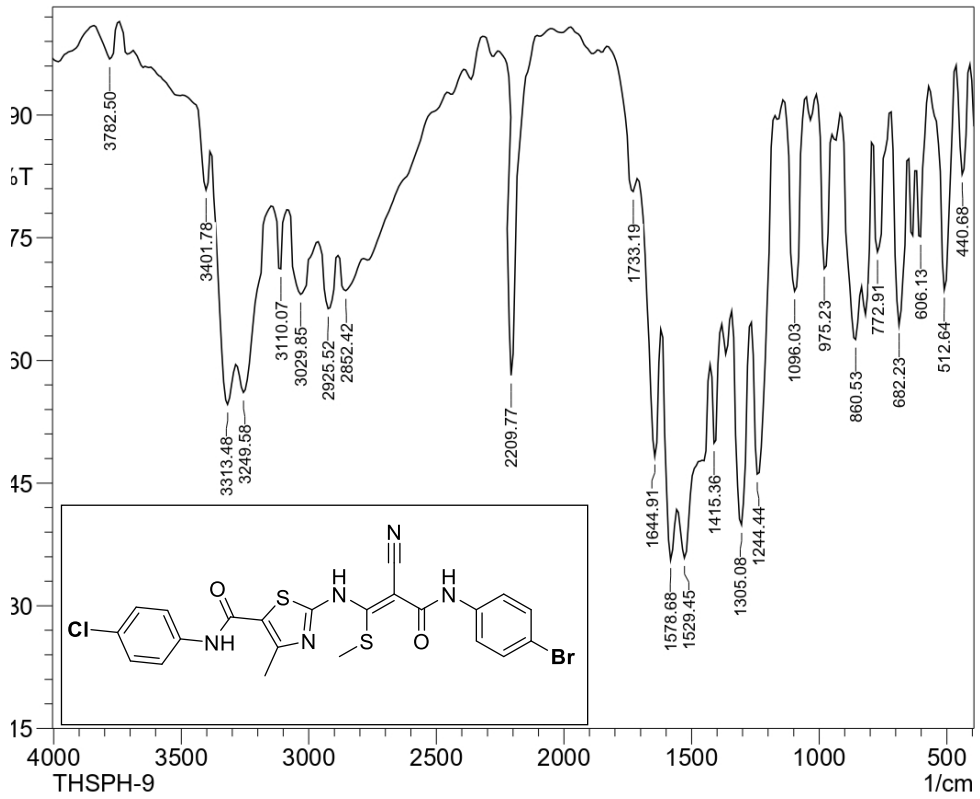

Fig. 24: Representative IR spectrum of compound **THSPH-9**

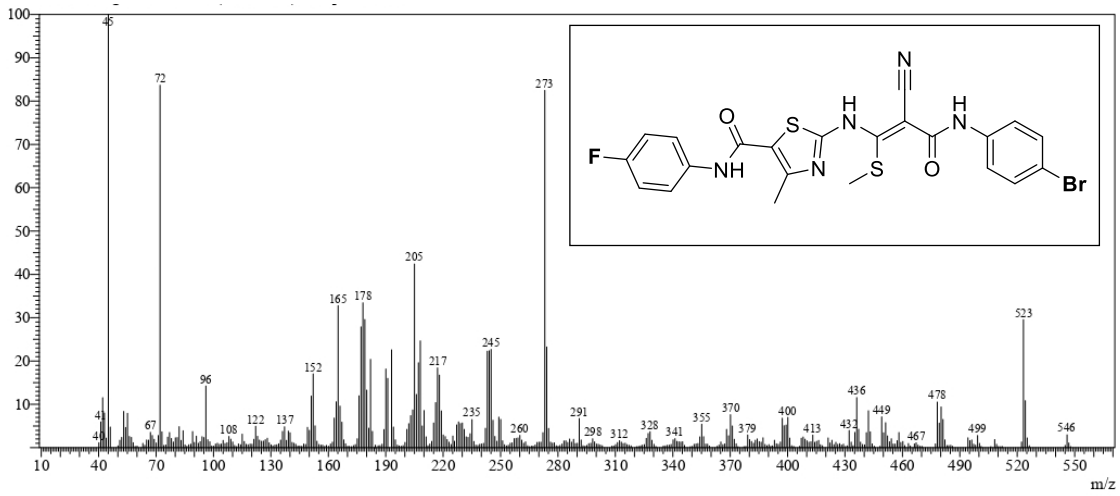

Fig. 25: Representative mass spectrum of compound **THSPH-10**

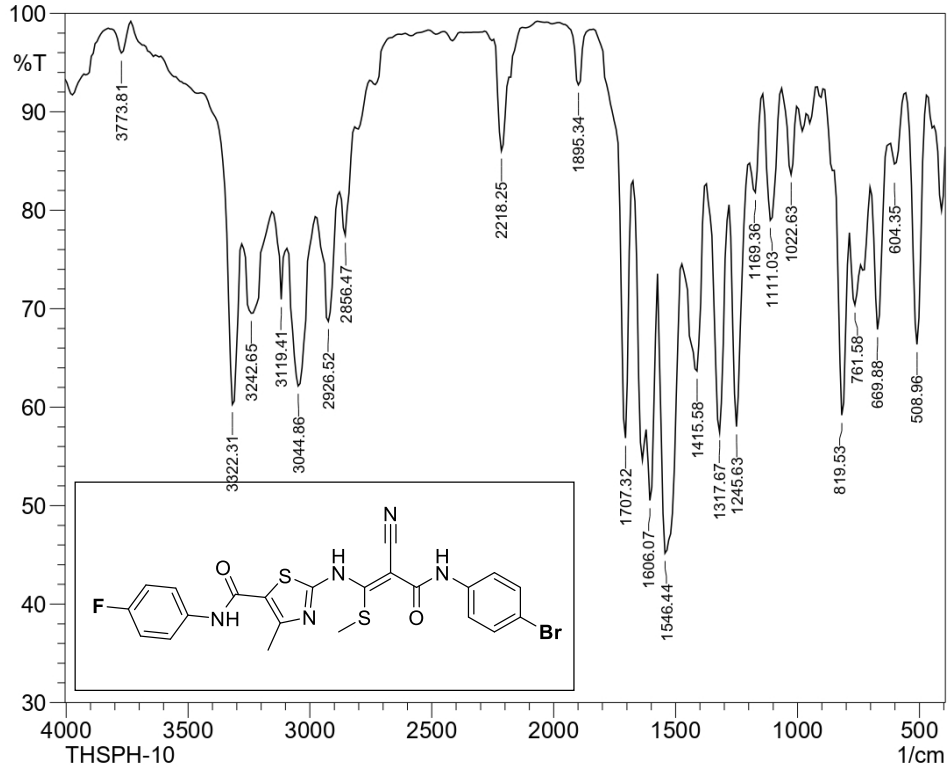

Fig. 26: Representative IR spectrum of compound **THSPH-10**

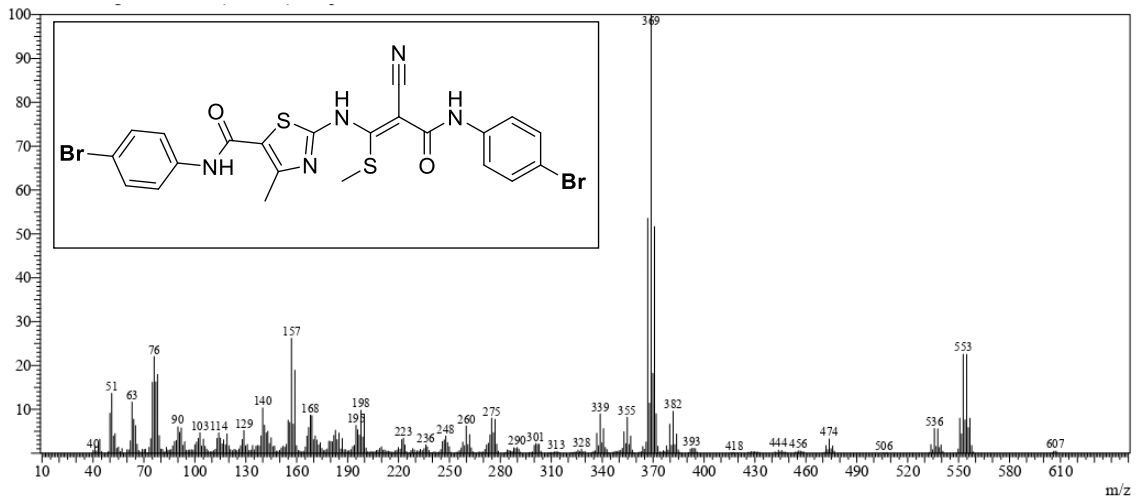

Fig. 27: Representative mass spectrum of compound **THSPH-11**

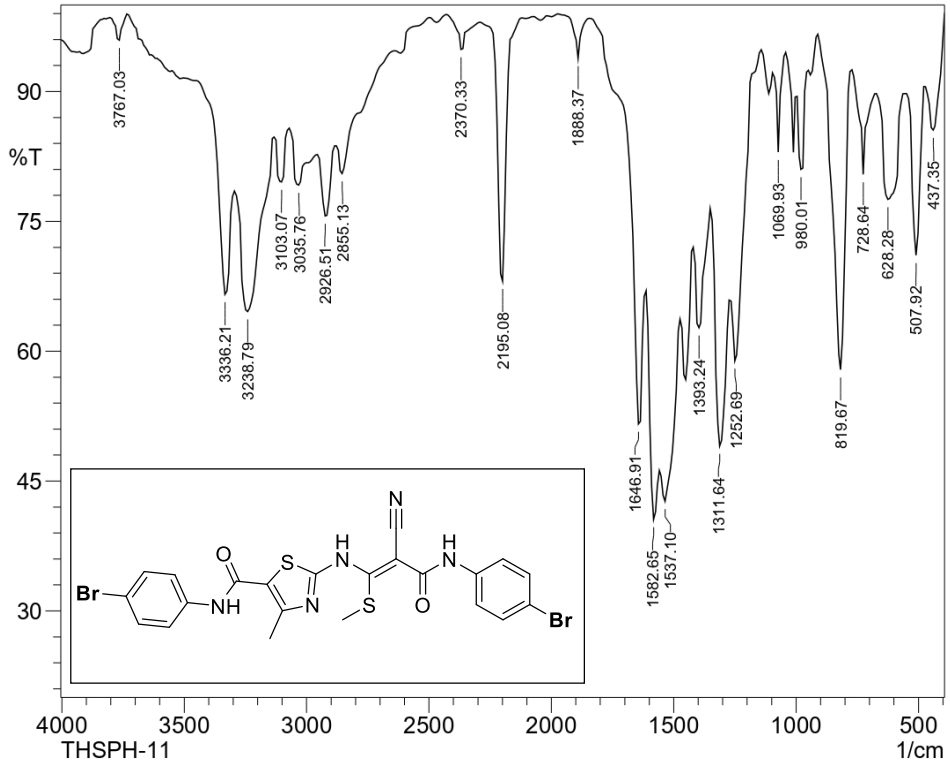

Fig. 28: Representative IR spectrum of compound **THSPH-11**

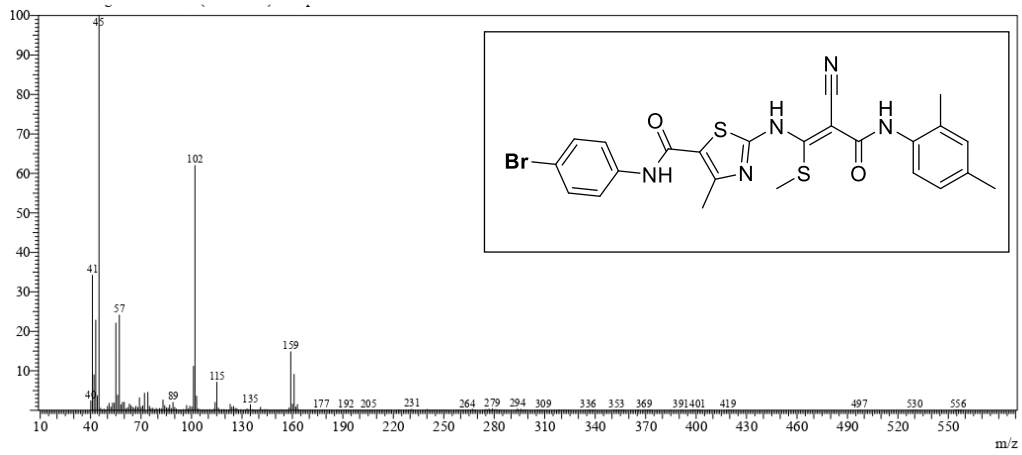

Fig. 29: Representative mass spectrum of compound **THSPH-12**

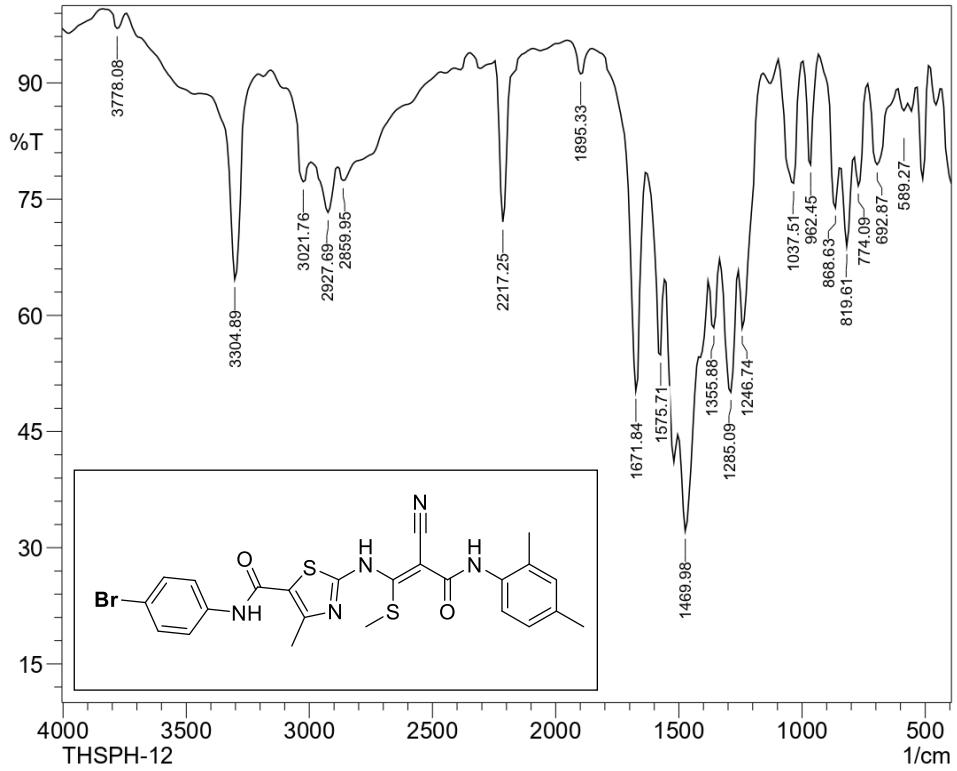

Fig. 30: Representative IR spectrum of compound **THSPH-12**

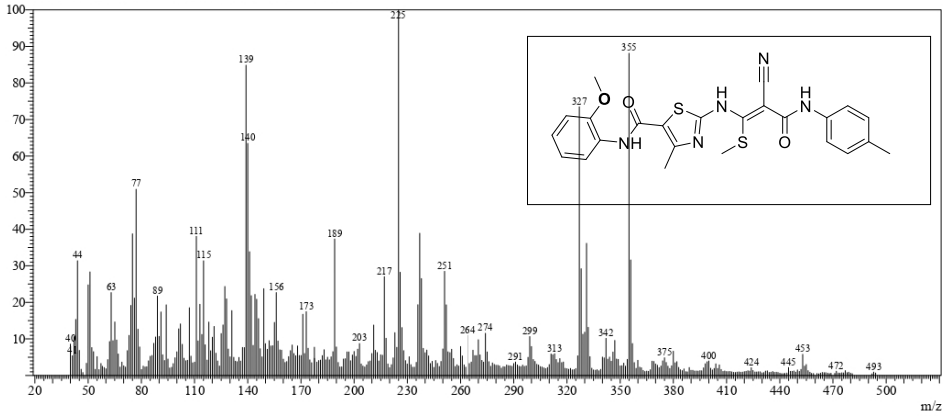

Fig. 31: Representative mass spectrum of compound **THSPH-13**

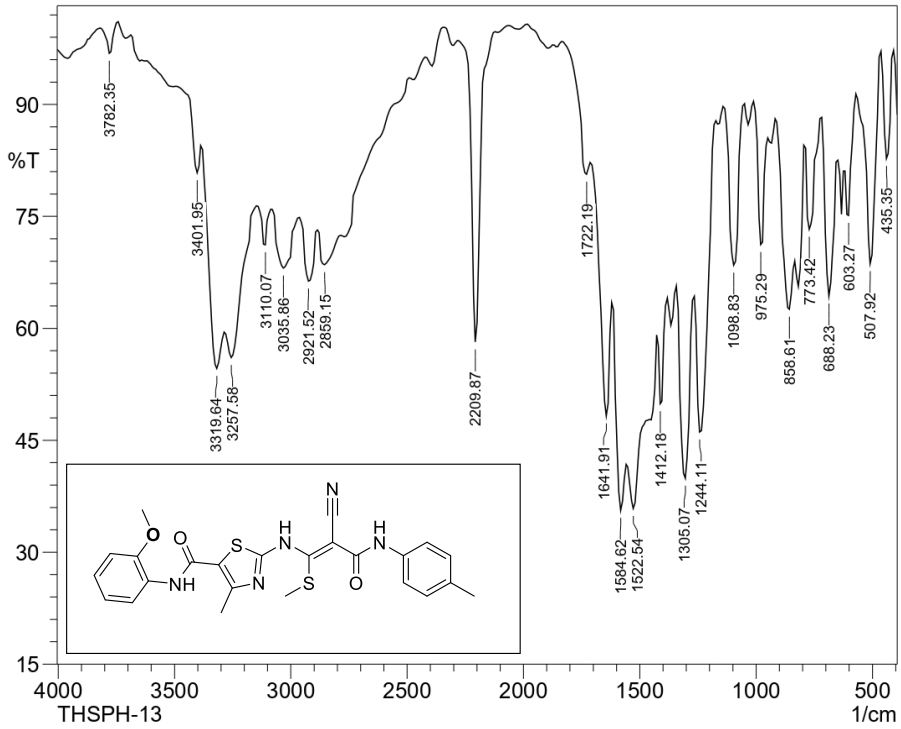

Fig. 32: Representative IR spectrum of compound **THSPH-13**

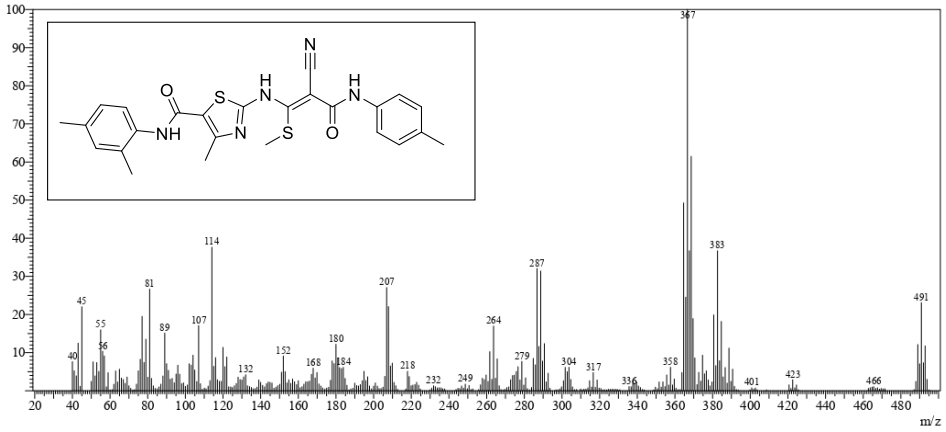

Fig. 33: Representative mass spectrum of compound **THSPH-14**

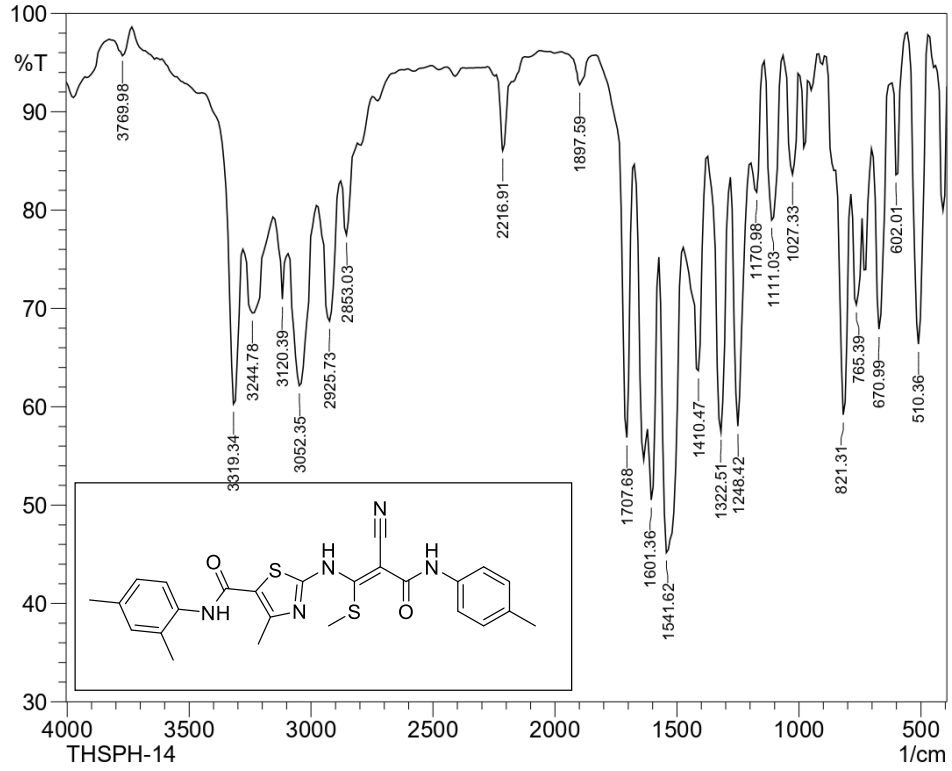

Fig. 34: Representative IR spectrum of compound **THSPH-14**

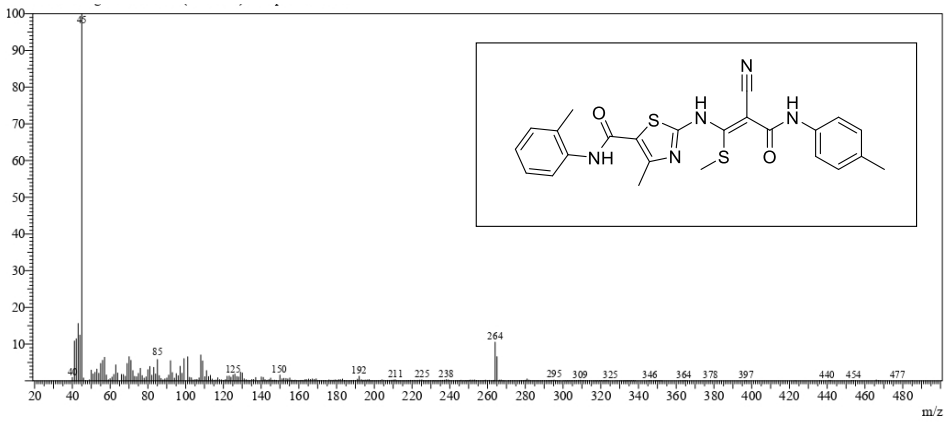

Fig. 35: Representative mass spectrum of compound **THSPH-15**

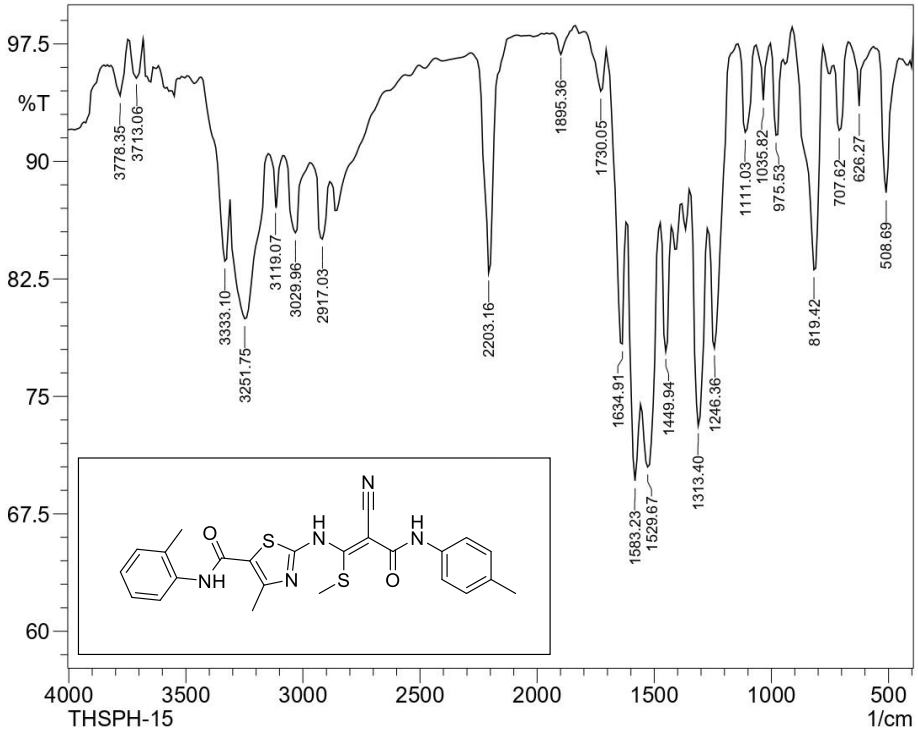

Fig. 36: Representative IR spectrum of compound **THSPH-15**